SYNTHESIS OF MAGNESIUM/B4C SURFACE COMPOSITE BY FRICTION STIR PROCESSING

A

Project Report

submitted in partial fulfillment of the requirement for the award of the degree of

MASTER OF TECHNOLOGY

In

PRODUCTION AND INDUSTRIAL ENGINEERING

By

SUMIT JOSHI
2K14/PIE/17

Under the guidance of

Mr. N. YUVRAJ
ASSISTANT PROFESSOR

DEPARTMENT OF MECHANICAL ENGINEERING
DELHI TECHNOLOGICAL UNIVERSITY
NEW DELHI-110042
2014-16

Department of Mechanical Engineering

Delhi Technological University

Delhi

CERTIFICATE

This is to certify that the thesis entitled **"Synthesis of Magnesium/B_4C Surface Composite by Friction Stir Processing"** submitted by **Sumit Joshi (2K14/PIE/17)**, during the session 2014-2016 for the award of M.Tech degree of Delhi Technological University, Delhi is absolutely based upon his work done under my supervision and guidance and that neither this thesis nor any part of it has been submitted for any degree/diploma or any other academic award.

The assistance and help received during the course of investigation have been fully acknowledged. He is a good student and I wish him good luck in future.

Mr. N. Yuvraj

Assistant Professor

Department of Mechanical Engineering

Delhi Technological University

ACKNOWLEDGEMENT

I like to express my deep sense of respect and gratitude to my project guide Mr. N. Yuvraj, Department of Mechanical Engineering, Delhi Technological University, Delhi for his invaluable and fruitful constructive suggestions and guidance that have enabled me to overcome all the problems and difficulties while carrying out multi-functionaries of the present investigation. I feel fortunate for the support, involvement and well wishes of my mentors and this is virtually impossible to express them in words. I also wish to express my gratitude to all the lecturers and staff members of the Mechanical Engineering Department for their help throughout the course.

SUMIT JOSHI
2K14/PIE/17
M.Tech (Production and Industrial Engineering)
Delhi Technological University

DECLARATION

I, **Sumit Joshi**, hereby certify that the work which is being presented in this thesis entitled **"Synthesis of Magnesium/B_4C Surface Composite by Friction Stir Processing (FSP)"**, is submitted, in the partial fulfillment of the requirements for degree of Master of Technology at Delhi Technological University is an authentic record of my own work carried under the supervision of **Mr. N. Yuvraj**. I have not submitted the matter embodied in this seminar for the award of any other degree or diploma also it has not been directly copied from any source without giving its proper reference.

SUMIT JOSHI
2K14/PIE/17
M.Tech (Production and Industrial Engineering)
Delhi Technological University

ABSTRACT

In the new era, cost saving is one of the target of aerospace and automotive industries. To achieve this, there is a requirement of the material having high strength to weight ratio. Magnesium is one of the materials which possess this property. Magnesium-based alloys have enormous potential for cost saving application due to their light weight combine with high specific strength and corrosion resistance, excellent stiffness and damping capacity, as well as good castability and favourable recycling capability. This report is concerned with the fabrication of surface composites. Surface composites are a group of modern engineered materials where the surface of the material is modified by dispersing secondary phase in the form of particles or fibers and the core of the material experience no change in chemical composition and structure. The potential applications of the surface composites can be found in automotive, aerospace, biomedical and power industries. Recently, friction stir processing (FSP) technique has been gaining wide popularity in producing surface composites in solid state itself. Magnesium and its alloys being difficult to process metals also have been successfully processed by FSP to fabricate surface composites. Friction Stir Processing (FSP) is a solid state joining process which uses a non consumable rotating tool inserted into the workpiece for heating and softening the material. This results in material severe plastic deformation resulting in improved mechanical properties and refined grain structure. Most of the research conducted on FSP is confined to aluminium alloys; limited study is done on FSP of magnesium based alloys.

In the present work, an attempt has been made to synthesize magnesium based alloy having composition Mg-4Al-3Zn-3Pb-3Sn-0.5misch metal (MM) and Boron Carbide (B_4C) micro sized particle surface composite using Friction Stir Processing (FSP). Mechanical properties such as hardness and wear resistance of the FSPed surface composites were evaluated and compared with the properties of base metal. The results indicated that B_4C particles were distributed uniformly in the Mg matrix and surface composite exhibited better hardness and wear resistance as compared to base metal.

CONTENTS

LIST OF TABLES

LIST OF FIGURES

CHAPTER-1

INTRODUCTION

Cast magnesium alloys are progressively replacing aluminium and steel in the aerospace and automobile industries and plastic in the electronic and computer industries due to low weight and good thermal and electrical conductivity. This increasing demand of magnesium alloys is due to its low density, high specific strength, good castability, weldability and machinability [1]. Among Mg-alloys, Mg-Al alloys are most promising for automotive industries because of their acceptable mechanical properties, good corrosion resistance and excellent cast-ability [5]. Magnesium alloys are finding increasing applications in industry mainly due to their high strength-to-weight ratio. However, most of magnesium alloys generally show poor creep resistance at elevated temperatures, which restrict their industrial applications. As a result, Mg–RE alloys (RE represents rare earth elements) are developed to meet the demand for high temperature usage. The addition of RE elements can produce thermally-stable second phases in the Mg matrix, leading to high strength and good creep resistance at high temperature. Also, the main drawback of using wrought Mg alloy is its poor formability at room temperature due to its Hexagonal Closed Packed (HCP) crystal structure; only three independent basal slip systems can be activated, all parallel to the slip plane (0001). Therefore, ductility enhancement is one of the key issues for the industrial application of magnesium alloys. It is well known that grain refinement is an effective way to enhance the mechanical properties of magnesium alloys. Fine grained structures have been successfully achieved by applying various techniques, e.g. grain refiners [2], altering, rapid solidification [3], spray co-deposition, recrystallization, and severe plastic deformation such as equal channel angular pressing (ECAP) [4].

Friction Stir Processing (FSP) is one of the severe plastic deformation (SPD) method which is based on the basic principles of Friction Stir Welding (FSW) invented by The Welding Institute (TWI) in UK in 1991 [6]. Compared with other SPD techniques, FSP is considered as an efficient and environmental-friendly technique since it can produce fine and uniform microstructure in a single pass without any additional heat-treatment. In the past few years, several studies have been conducted to understand the effect of FSP on the microstructure and properties of Mg-Al-Zn (AZ) alloys. It is reported that FSP results in remarkable grain refinement and significant breakup and dissolution of the coarse, network

like secondary eutectic phase β-$Mg_{17}Al_{12}$ distributed at the grain boundaries, which significantly improves the tensile properties of the casting [7].

Though FSP was initially employed for microstructural refinement of aluminum and magnesium alloys, it is a very attractive process for also fabricating composites. Mishra et al. [8] fabricated the SiC/Al surface composites by FSP, and indicated that SiC particles were well distributed in the Al matrix, and good bonding with the Al matrix was generated. There are numerous conventional methods for fabricating surface composites such as powder metallurgy, laser melt treatment, plasma spraying, stir casting etc but these techniques lead to the deterioration of composite properties due to interfacial reaction between reinforcement and the metal matrix [10]. These techniques involve the material transformation from solid to liquid or vapour state during the process as compared to solid state processing technique. Moreover, precise control of processing parameters is required to obtain desired microstructure in surface layer after solidification. FSP is one of the solid state processing techniques which have proved its potential in fabrication of all variants of surface composites with little or no interfacial reaction with the reinforcement. The potential applications of the surface composites can be found in automobile, aerospace, marine and power generation industries. Magnesium and its alloys being difficult to process metals have been successfully processed by FSP to produce surface composites.

CHAPTER-2

LITERATURE REVIEW

2.1 Friction Stir Processing

The Friction stir processing is a solid-state welding; microstructural modification technique using a frictional heat and stirring action. It was developed by Mishra and Z.Y. Ma [8] as a generic tool for microstructural modification based on the basic principles of FSW. In this case, a rotating tool is inserted in a monolithic workpiece for localized microstructural modification for specific property enhancement. For example, high-strain rate superplasticity was obtained in commercial 7075Al alloy by FSP. Furthermore, FSP technique has been used to produce surface composite on aluminum substrate, homogenization of powder metallurgy aluminum alloy, microstructural modification of metal matrix composites and property enhancement in cast aluminum alloys.

Friction stir processing is a special technique to improve the microstructure in the solid state by using the heat from friction for the aluminum-casting and magnesium alloy. The mechanical properties such as ultimate tensile strength of friction stir processing are improved due to the grain refinement of the microstructure.

2.1.1 Working Principle of FSP

The schematic illustration of FSP operation is shown in fig. 2.1. First of all, the non-consumable cylindrical tool is rotated to a predetermined RPM. After that, the tip of the rotating tool is plunged into the workpiece which performs two primary functions: (1) Heating and (2) Deformation of workpiece material. The tool's shape consists of a small diameter pin which is fully inserted into the metal, and a concentric, larger diameter shoulder which is intended to prevent upward displacement of the material at the surface of the workpiece. As the tool penetrates the surface, the rotating pin creates frictional and adiabatic heating. This combination of heating softens the material so that the tool can further penetrate the material. As the tool rotates, it induces a stirring action and material flows around the pin. The depth of penetration is controlled by the tool's shoulder and the length of the pin. Now, the shoulder makes contact with the material's surface. This expands the hot zone due to heating caused by the rotating tool shoulder. The shoulder prevents the upward flow of material caused by the stirring action of the pin results in forging action on the deforming

material. When the tool is fully inserted into the workpiece, it then traverses across the metal at a specific rate, IPM (inches per minute).

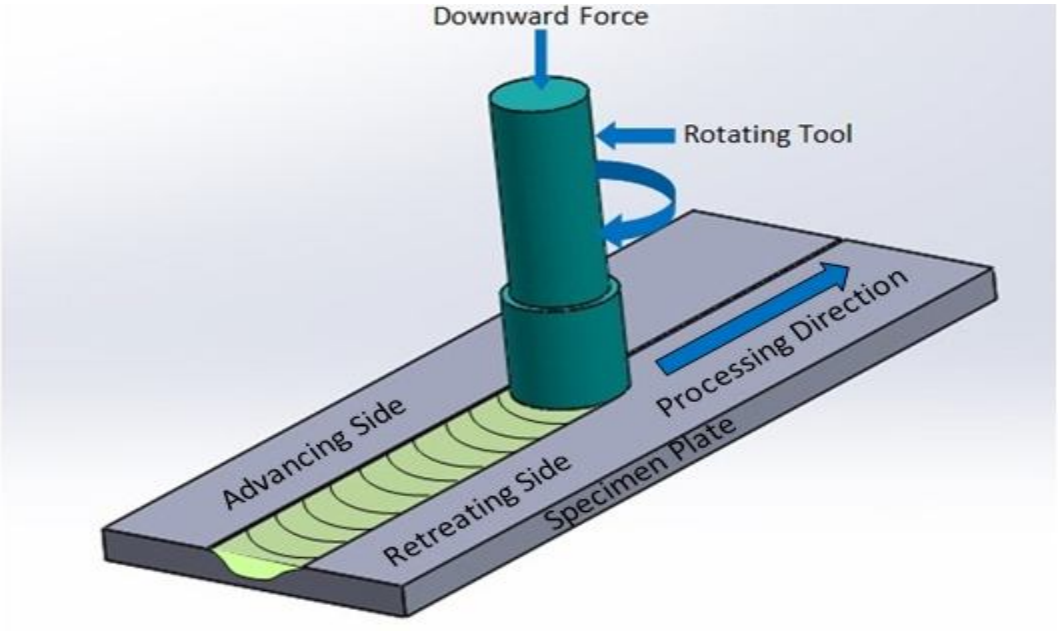

Figure 2.1 Schematic Illustration of Friction Stir Processing Technique.

During FSP, the rotating tool provides a continual hot working action, plasticizing the metal within the narrow region surrounding the pin, while transporting the metal from the leading face (advancing side) of the pin to its trailing edge (retreating side). It is important to note that the metal never melts. The peak temperatures achieved in this process are typically 80 to 90 percent of the melting temperature. After the tool passes by, the processed material cools and exhibits a refined and homogenized microstructure. Essentially, FSP is a thermomechanical metal working process that changes the local properties with minimal influence on the properties in the rest of the material [8].

2.1.2 FSP Process Parameters

FSP includes following types of process parameters which affect microstructural characteristics and mechanical properties of magnesium alloy. These are

- **Tool Geometry:** - In FSP, tool performs two functions of localized heating and material flow. It includes tool pin shape (threaded cylindrical or square) and shoulder shape (concave or convex).
- **Welding Parameter:** - It includes tool rotational speed and tool traverse speed along the welding line. The tool rotation results in stirring and mixing of softened materials

around the pin, and the tool translation moves them from the front to the back of the pin and finishes the weld.

- **Tool tilt or tilt angle**
- **Tool penetration depth**

2.1.3 Processed Region Terminology

It is also common to discuss the processed area in FSP with specific terminology. As shown in fig.2.2, three distinct zones are identified after FSP of aluminium alloy i.e., Nugget or Stirred Zone (SZ), Thermo Mechanically Affected Zone (TMAZ) and Heat Affected Zone (HAZ). The microstructural changes in various zones have significant effect on postweld mechanical properties.

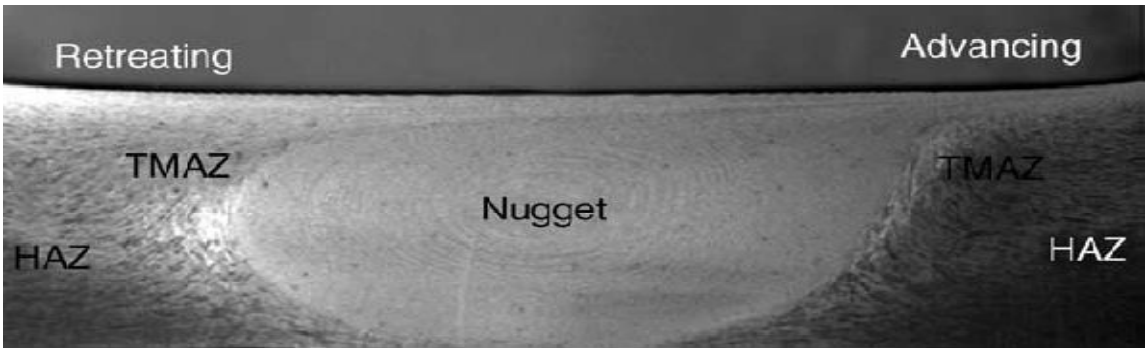

Figure 2.2 Various zones in the cross-section of FSP 7075Al-T651 [9].

Intense plastic deformation and frictional heating during FSW/FSP result in generation of a recrystallized fine-grained microstructure within stirred zone. This region is usually referred to as nugget zone (or weld nugget) or dynamically recrystallized zone (DXZ). Unique to the FSW/FSP process is the creation of a transition zone—thermo-mechanically affected zone (TMAZ) between the parent material and the nugget zone, as shown in Fig.2.3. The TMAZ experiences both temperature and deformation during FSP. The TMAZ is characterized by a highly deformed structure. The parent metal elongated grains were deformed in an upward flowing pattern around the nugget zone. Beyond the TMAZ there is a heat-affected zone (HAZ). This zone experiences a thermal cycle, but does not undergo any plastic deformation.

2.2 Material Properties and Designation: Magnesium Alloy

Magnesium, with a density of 1.74 g/cm^3, is the lightest of all structural metals. It is two third of its counterpart aluminium (density: 2.7 g/cm^3) and one third of steel (density: 7.8 g/cm^3). High thermal conductivity, damping capacity and machinability makes Mg alloy advantageous for aerospace and automotive applications. However, the symmetry of the Hexagonal Close-Packed (HCP) crystal structure has the limited numbers of independent slip systems, resulting in poor formability and ductility at room temperature.

2.2.1 Magnesium alloy designation

No international code for designating Mg alloys exists, but can use ASTM system designated by two capital letters followed by two or three numbers.

- The letters stand for the two major alloying elements
    1. First letter stands for the highest amount.
    2. Second letter stands for the second highest amount.
- The numbers stand for the amount of the two major alloying elements
    1. First number following the letters stands for the wt% of the first letter element.
    2. Second number stands for the wt% of the second letter element.

Table 2.1

Coding for Mg based alloys

Abbreviation letter	Alloying element	Abbreviation letter	Alloying element
A	Aluminium	P	Lead
C	Copper	Q	Silver
D	Cadmium	R	Chromium
E	Rare earth	S	Silicon
F	Iron	T	Tin
H	Thorium	Z	Zinc
K	zirconium	M	Manganese

2.3 Magnesium Based Alloy Surface Composites

Surface composite is a multiphase material, that is artificially made, in which the surface of the material is modified by incorporating secondary phase in the form of particles and fibres. Magnesium alloys application is limited due to their poor creep resistance at high temperatures, low strength, low modulus and wear resistance. Therefore, reinforcement is added to improve the properties of the base metal. The most commonly used reinforcements in fabrication of Mg surface composites are Silicon Carbide (SiC), Aluminium Oxide (Al_2O_3), and Titanium Carbide (TiC), etc. SiC reinforcement increases the ultimate tensile strength, yield strength, hardness, ductility and wear resistance of Mg and its alloys. Reinforcement of TiC particles lead in improvement of yield strength tensile strength and elastic modulus significantly, while the ductility is reduced to some extent. Reinforcement of Al_2O_3 induces good creep resistance, compressive strength. The addition of Boron Carbide (B_4C) in magnesium matrix increases the interfacial bonding strength, flexural strength of hybrid composite, hardness and wear resistance [11]. Some of the well established conventional methods developed for fabricating Mg based alloy composites include stir casting, squeeze casting and powder metallurgy. Other than these techniques in-situ synthesis, mechanical alloying, pressureless infiltration, gas injection, and spray forming are also newly developed fabrication techniques. All these techniques include liquid phase during processing which results in oxidation and entrapment of gases and inclusions since Mg is very reactive metal compared to aluminium. Therefore, no commercial use of stir casting has been reported on magnesium matrix composites. The excessively high pressure in squeeze casting leads to severe damage to the reinforcement particle and reduce the mechanical properties of the composites. Powder metallurgy is a costly technique since it involves alloy powders that are generally more expensive than bulk material, and involves complicated processes during the material fabrication [12]. The non uniform dispersion of the reinforcement particles is still a major issue in these techniques. So, attention is paid on a newly surface modification technique so called Friction Stir Processing (FSP) which is more advantageous than the conventional technique. FSP is a solid state technique which does not involve any liquid phase during processing thus eliminating gas defects and also it leads to uniform distribution of reinforcement particles.

2.4 Literature Study

In this section, various investigations regarding Friction Stir Processing (FSP) of Magnesium alloys are presented. It is divided in two sub sections, one section is concerned with the simple FSP of non ferrous alloys especially Mg. Another section is concerned with the application of FSP i.e. fabrication of Metal Matrix Composites (MMCs) by FSP.

2.4.1 FSP of non ferrous alloys

To study the FSP effect, different process variables are employed such as FSP tool rotational and traverse speed, no. of FSP passes, tool geometry, direction of tool rotation etc.

Darras et al. [13] studied various samples of commercial AZ31B-H24 magnesium alloy sheets which were friction stir processed with a single pass at different combinations of rotational (1200-2000 rpm) and translational (20-30 in/min) speeds. The effect of different combinations on temperature profiles, microstructure and hardness is presented in their study.
Temperature: - Result revealed that that peak temperature increases as the rotational speed increases and translational speed decreases.
Microstructure: - For study of microstructure two samples were taken, which were processed at same rotational speed of 1200 rpm and different translational speed of 22 and 25 in/min. Result exhibited that that FSP produced a more homogeneous microstructure compared to as cast material. Also FSP refined the microstructure from an average grain size of about 6μm to a grain size of about 3-4μm.
Hardness: - Result shows that hardness has inverse relation with rotational speed and direct relationship with the translational speed.

Wen et al. [14] treated Cast AZ31 magnesium alloy by the single-pass and two pass friction stir processing (FSP), respectively, and the microstructure and mechanical properties were investigated. The plates with 5 mm in thickness were subjected to the single-pass and two-pass FSP at a stir tool rotation rate of 950 r/min and a traverse speed of 30 mm/min, respectively. The two pass FSP was adopted with a 100% overlap and the same forward direction as the single pass FSP. Results revealed that

- FSP caused the breakup and dissolution of the coarse eutectic β-$Mg_{17}Al_{12}$ phase into the magnesium matrix, and the remarkable grain refinement and homogenization. The average grain sizes of the single-pass and two-pass FSP specimens were about 4.2 and 1.6 μm in the SZ, respectively.

- There was no obvious preferential orientation in the parent material and single-pass FSP specimen while the two-pass FSP specimen exhibited the preferential grain orientation, and (0002) plane showed a strong tendency to be arranged parallel to the plate surface.
- The ultimate tensile strengths of the single pass and two-pass FSP specimens increased by 43 and 82 MPa, and elongations increased by 4.3% and 11.9%, respectively, as compared to that of the parent material. The fracture surface of the cast AZ31 alloy exhibited a typical ductile dimple-facture after FSP.

Valle et al. [15] analyzed the relationship of microstructure and mechanical properties in a friction stir processed (FSP) AZ91 magnesium alloy. A rotation rate of 700 rpm in clockwise direction, a traversing speed of 120 mm/min, and a tool tilt angle of 1.5° were used. In order to control the heat sink during the FSP processing, two experimental set-ups were developed, the heat insulator system with the preheated samples and the cooling system. Results shows that

- The control of the heat sink and sample temperature allows for FSP samples of good quality, enhancing the grain size refinement in the stirred zone down to values close to 0.5 μm after a second pass.
- Results on yield stress at room temperature show a sharp decrease in the Hall–Petch slope related to a favorable orientation for slip of the basal planes. Noticeable changes in ductility were explained in terms of the grain size and texture effects on work hardening behavior. It was shown that favorable texture in FSP2 samples induces a stage with a smoothly linear decrease of the work hardening rate and high ductility.
- Moreover, a grain size decrease, obtained in samples FSP3 and FSP4 induces a stage of constant work hardening, but with a low rate, insufficient to obtain a high elongation. The use of different FSP routes promotes microstructural changes useful for designing a high strength or, alternatively, a high ductility material.
- At high temperature grain boundary sliding is responsible of superplastic behavior.

Feng and Ma [7] investigated the effect of FSP on microstructure and mechanical properties of AZ91D Mg alloy along with subsequent aging and find that FSP combined with aging is an effective approach to enhance the mechanical properties of cast AZ91 alloy. Results revealed that FSP leads to development of 430^0C temperature which results in significant breakup and dissolution of the coarse eutectic β-$Mg_{17}Al_{12}$ network present at the grain boundaries in the Mg matrix and remarkable grain refinement (15 μm), thereby improving

significantly the tensile properties, in particular ductility. Moreover, Post-FSP aging resulted in continuous precipitation of fine β-$Mg_{17}Al_{12}$ particles, thereby increasing the yield strength from 73 MPa (as cast) to 177 MPa, UTS from 111 MPa (as cast) to 337 MPa; and decreasing the ductility.

DU Xing-hao and WU Bao-lin [16] produced ultrafine-grained microstructure in AZ61 Mg alloy by FSP assisted by rapid heat sink. In order to obtain rapid cooling during FSP, liquid nitrogen cooling method was used. Ultrafine grained microstructure appeared in the bottom of nugget zone. The mean grains refined to less than 300 nm. Also, Friction stir processing drastically increases the microhardness of AZ61 to the mean value of 120-130 Hv which was almost three times higher than that of the as cast AZ61.

Some studies are also done on the effect of FSP parameters on the formation of FSP defects such as pin hole, tunnel defect, piping defect, surface cracks etc. Babu et al. [17] studied the effects of FSP parameters such as tool traverse speed (40, 75, 105 mm/min), tool rotational speed (1000 rpm and 1200 rpm) and tool shoulder diameter (18 and 24 mm) on the microstructure and mechanical properties of FSPed extruded AZ31B alloy. It was observed that with 18 mm tool shoulder diameter, tunnelling defect was present in the stirred zone for most of the processing parameters. This may be due to the less heat generation between at the pin workpiece interface and also at the tool shoulder and workpiece interface. Defect free FSPed zone was observed when the minimum FSP parameters were 24 mm shoulder diameter, 75 mm/min traverse speed and 1000 rpm. FSP leads to grain refinement in the nugget region with an average grain size of less than 10 µm. Further, FSP leads to increase in percentage elongation from 1.2 to 1.82 times of the base metal.

Arora et al. [18] examined wear behaviour of an Mg alloy AE42 under as-cast as well as friction stir processed conditions. Wear tests were performed in a pin-on disc configuration using Universal Tribometer. The load range was varied from 5 to 20N, whereas sliding velocity from 0.33 to 3m/s. Results shows that

- For the range of normal loads and sliding velocities investigated, friction stir processed (FSPed) AE42 alloy demonstrated reduced wear rate under all the conditions.
- The major factors that contributed to the reduced wear rates for FSPed AE42 alloy were found to be microstructural refinement resulting in higher hardness, greater work hardening capability and improved ductility. It was found that maximum mass loss/sliding distance (wear rate) occurred at highest load and lowest velocity. Moreover,

wear rate was found to decrease with decrease in load and increase in sliding velocity for most of the cases.

- Abrasive and oxidation were found to be dominant wear mechanisms in the low velocity regime. At intermediate sliding velocity, delamination also became significant along with abrasion and oxidation. The major wear mechanisms at high velocities were found to be plastic deformation along with delamination.
- The as-cast alloy has shown higher value of coefficient of friction (COF) than the FSPed alloy at 5N as well as at 10N loads and all sliding velocities. However, at 20N load and 0.33 m/s velocity, the FSPed alloy has shown higher COF than the as-cast alloy.This may be attributed to the higher work hardening of the FSPed alloy at 20N load and 0.33 velocity.
- The subsurface analysis revealed higher work hardening tendency at low sliding velocities. This may be attributed to the dominance of thermal softening effect over work hardening at higher velocity because of high surface temperatures.

Magnesium alloys generally shows poor creep resistance at elevated temperature due to which their application is limited in high temperature applications. For this, Rare Earth (RE) elements are added to Mg alloys to produce thermally stable second phase in the Mg matrix which leads to high strength and high creep resistance at elevated temperature. Cao et al. [19] studied microstructure evolution and its effect on mechanical properties of Mg–Nd–Y alloy during normal friction stir processing (NFSP) and submerged friction stir processing (SFSP). Plates with 6 mm thickness were machined from the cast billets and then subjected to single-pass NFSP and SFSP at a rotation rate of 800 rpm and a traverse speed of 40 mm/min. Results shows that:

- After NFSP and SFSP, α-Mg dendrites in the as-cast alloy are greatly refined and the coarse $Mg_{12}Nd$ phases are broken into small particles. Due to the rapid cooling effect during SFSP, the average grain size of SFSP specimen (1.9μm) is finer than the NFSP specimen (2.7μm). Coarse grain band structure is formed in the NFSP specimen, while this structure is rarely found in the SFSP specimen.
- The as-cast alloy exhibited the lowest UTS of 178 ± 3.5 MPa, the lowest YS of 172 ± 3 MPa and the lowest elongation of 3.4 ± 0.5%. After NFSP and SFSP, the UTS, YS and elongation were increased to 291 ± 4.6 MPa, 270 ± 5 MPa, 7.5 ± 0.5% and 297 ± 6.9 MPa, 281 ± 3.9 MPa, 20.3 ± 1.8%, respectively. Due to the microstructure refinement,

the mechanical properties of the alloy were improved greatly after FSP, and the SFSP specimen possesses the best properties due to its finest grain size and homogenized microstructure.

Zheng et al. [20] studied the FSP effect on microstructure and mechanical properties of NZ20K extruded alloy having composition Mg-2.0Nd-0.3Zn-1.0Zr. FSP resulted in significant breakup and dissolution of intermetallic phase $Mg_{12}Nd$ in the Mg matrix. The microstructure of the SZ is characterized by fine and equiaxed α-Mg grains, since complete dynamic recrystallization takes place during FSP. This results in reduction of average grain size from about 20.6 μm in as-extruded condition to about 3.8 μm in SZ by FSP with three passes. Moreover, with the increase of pass, the average grain size in SZ reduces firstly and then increases. However, tensile properties results were not like hardness results since tensile properties depend upon various factors which include grain size, amount and morphology of secondary phase, amount of dislocation density, defect, and crystallographic texture etc. In 1 pass FSP, texture modification during FSP was not dominant compared to 3 pass and 5 pass FSP and had negative effect regarding Yield Strength (YS) which leads to decrease in YS of 3 pass and 5 pass FSPed material (117 MPa) compared to parent metal (124 MPa) and 1 pass FSPed material (141 MPa). Hardness was improved from 65 Hv (parent metal) to 82 Hv (1, 3 and 5 FSP pass) because both grain refinement and texture modification had positive effects.

Among the non ferrous alloys, most of the FSP study is done on aluminium alloy. Saini et al. [21] studied the effect of input process parameters of FSP to enhance the mechanical and tribological performance of the cast hypereutectic Al-17%Si alloy. The input process parameters used for FSP were selected by number of pilot experiments i.e. fixed tool rotation speed (TRS) of 664 rpm and variable welding speed of 26, 40 and 60 mm/min. Major findings were:

- The significant refinement of eutectic and coarse primary Si particles and improved distribution of Si particles in the Al matrix takes place as a result of FSP in cast Al-17% Si alloy. FSP recorded for generating fine grains of 2–4μm approximately in cast Al-17%Si alloy samples and input process parameters of FSP did not exert a significant effect on the grain size.
- FSP increased UTS (Ultimate tensile stress) of cast Al-17% Si alloy. FSP samples showed 1.26 to 1.35 time higher strength than base material. Moreover, FSP increased

% elongation of cast Al-17% Si alloy from < 2 % to about 9 % and the mirohardness. An increase in welding speed increases the microhardness of cast Al-17% Si alloy.

- Mechanical properties results the optimize parameter for FSP of cast Al-17% Si alloy were TRS of 664 rpm and welding speed of 60 mm/min.

Chainarong et al [22] improved the mechanical properties of SSM 356 aluminum alloys by friction stir processing. The parameters of friction stir processing for SSM 356 aluminum alloys were studied at three different travelling speeds: 80, 120 and 160 mm/min under three different rotation speeds 1320, 1480 and 1750 rpm. Main findings were:

- The surface of specimen is improved by the friction stir process. Macrostructure through a friction stir processing showed a homogeneous appearance as well. No defective part was found. The surface of stirred is smooth. The microstructure after the friction stir processing at all conditions have a very refined structure, which consists of a silicon particles in aluminum alloy matrix uniformly distributed throughout the area to be stirred. However, investigation did not find any defects with the stirred.
- The hardness of the area was influenced by the thermal both retreating and advancing with increased hardness for all experimental conditions compared to that of base metal. But for the stir zone, the hardness can be either increased or decreased. The condition that increased the hardness is travelling speed at 120 and 160 mm/min with any rotation speed. The condition that reduced the hardness was travel speed at 80 mm/min with any rotation speed.
- The highest hardness, obtained at 1750 rpm with travel speed at 160 mm/min, is equal to 64.55 HV, an increase of 59.07% compared to the base metal.
- The average maximum tensile strength after using FSP was equal to 188.57 MPa, an increase of 11.8% compared to the base metal. It was found that the conditions providing strength to pull up the average was at the speed around the 1750 rpm and at the travel speed at 160 mm/min.

Karthikeyan et al. [23] investigated the effect of traverse speed of and rpm on the microstructure and mechanical properties of cast aluminium 2285 alloy. Samples were FSPed at three combinations of traverse speed 10, 12 and 15 mm/min and rpm of 1400 and 1800. Initially, authors concluded that FSP leads to elimination of casting defects like porosity, large sized grains and inhomogeneous grain structure present in the parent metal for all three combinations. With the increase in tool rpm, for a specific traverse speed, improved

mechanical properties were observed. Increased tool rotation rates resulted in enhanced mechanical properties due to reduced porosity and grain size. This is because at higher tool rotation rates, an increased frictional heating and stirring is present which creates a higher temperature in the nugget zone. This rise in temperature causes a greater refinement of grains with more thorough material mixing and a uniform distribution of the grains in the parent material, thus enhanced mechanical properties were observed. An increase in feed rate, for a particular speed reduces the time of exposure of material to increased temperatures, thus comparatively less refined grains and a slight decrease in output, though considerably higher than parent material. Finally, samples processed at a combination having traverse speed of 12 mm/min and 1800 rpm rotational speed were found to have better mechanical properties such as microhardness, yield strength, UTS and % elongation.

Aktarer et al. [24] examined the effect of two-pass FSP on the microstructural evolution, mechanical properties and impact toughness of as-cast Al–12Si alloy. FSP leads to the fragmentation of needle-shaped silicon plates into the smaller and more uniformly distributed particles inside nugget zone (NZ). The average length of eutectic Si particles decreases from 27±23 μm in the as-cast state to about 2.6±2.4 μm in the FSPed state due to the breaking of eutectic Si particles in the direction of length during FSP. Further, FSPed sample exhibits a tensile strength of about 215MPa and yield strength of about 131MPa, which was about 29% and 20% higher than those of as-cast alloy, respectively. Elongation to failure of the alloy increases from 3.4% in the as-cast state to about 25% after FSP (almost 7.4 times higher). Also, impact toughness of the as-cast alloy increases almost 7 times from 1.2J/cm² to about 8.3J/cm² after FSP. This improvement in all properties was mainly attributed to the refinement and morphological changes in eutectic silicon particles.

Mahmoud and Mohamed [25] studied the effect of FSP on the microstructural, mechanical and tribological characteristics of as-cast A413 aluminum alloy. Here, FSP was conducted using vertical milling machine at three different tool rotational speeds, typically, 900, 1120, and 1400 rpm and three different traverse speeds of 20, 40 and 63 mm/min. Results revealed that FSP greatly improved the microstructural properties of the as-cast A413 Al alloy by eliminating structural defects such as porosity. Moreover, the sizes of both coarse α-Al primary grains and coarse silicon fakes were significantly reduced by FSP. Also, the average size of the primary α-Al grains and Si particulates, at the center of FSPed regions, increases with increasing tool rotational speed and/or reducing tool traverse speed. The FSPed longitudinal tensile specimens exhibited better mechanical properties than the as-cast A413

Al alloy. Increasing the tool rotational speed and/or reducing the traverse speed reduce the ultimate and yield strengths, but improve the ductility, of the FSPed specimens. The ductility of the FSPed tensile longitudinal tensile samples is better than the ductility of the as-cast A413 Al alloy. FSP significantly improved the dry sliding wear resistance of the as-cast A413 Al alloy. However, the wear resistance was found to be reduced by increasing the tool rotational speed and/or reducing the traverse speed.

2.4.2 FSP Application of Fabrication/Synthesis

One of the most important applications of friction stir processing is to produce Metal Matrix Composites (MMCs). MMCs are very useful in automotive, aerospace, biomedical and power industries. Fabrication of MMCs is done on the surface as well as on the material as whole. In MMCs, secondary phase particles are introduced in the base metal as reinforcement to improve the properties such as specific strength, wear resistance, fatigue resistance. Surface MMCs contain dispersed secondary phase particles at the surface alone and core of the material is unaffected. There are some conventional techniques for fabrication of surface MMCs such as laser melt treatment, plasma spraying and centrifugal casting. Various studies revealed that these techniques lead to interfacial reaction between the parent metal and the composite due to the involvement of liquid phase during processing. In addition, precise control of processing parameters is required to obtain desired microstructure in surface layer after solidification. In the following discussion, we will find that FSP is an effective technique for fabrication of surface composites. Also, FSP resulted in improvement of mechanical and tribological properties. FSP is a solid state technique which does not involve liquid phase during processing compared to other fabrication techniques.

2.4.2.1 FSP of Magnesium based alloys surface composites

Most of the FSP study is confined to AZ series of the magnesium alloy. Commonly used reinforcements for fabrication are Titanium Carbide (TiC), Silicon Carbide (SiC), Aluminium Oxide (Al_2O_3), and Boron Carbide (B_4C) etc. Mostly, secondary phase particles are introduced in the matrix by groove filling and closing method which involves closing of groove with pinless FSP tool before doing FSP. This method is having the less possibility of escape of reinforcement particles. Morisada et al. [26] successfully dispersed the Multi-walled carbon nanotubes (MWCNTs) in AZ31 matrix by FSP. After doing FSP, their findings were:

- Dispersion of MWCNTs particles in AZ31 matrix depend on the travel speed of the rotating tool. Lower transverse speed exhibited good distribution of reinforcement particles in the Mg alloy matrix since it gives enough time for heat flow to produce desired viscosity in the matrix. A good dispersion was obtained for the sample FSPed at 25mm/min and 1500 rpm.
- Grain refinement due to FSP and extreme high strength of MWCNTs resulted in increase of microhardness of the composites. Maximum microhardness obtained was 78 Hv compared to 55 and 41 Hv of FSPed without reinforcement and as cast alloy respectively.
- Also, pinning effect exhibited by MWCNTs enhanced mechanical properties due to decrease in grain growth of AZ31 matrix.

Morisada et al. [27] also produced SiC/AZ31 surface composite by FSP. SiCp leads to grain refinement after FSP through recrystallisation process. Due to grain refinement by SiC particles and high hardness of particles, microhardness of stir zone with SiC particles is large compared to parent Mg alloy and FSPed Mg alloy. Fine grain structure of AZ31 obtained by FSP becomes unstable at high temperature while that of AZ31 having SiC particles was not affected by heat treatment process.

Number of FSP passes affects the grain distribution during FSP. Lee et al. [28] fabricated AZ61/SiO_2 nanocomposite by FSP. After FSP, the nano-SiO_2 particles were observed to be clustered in a size ranging from 0.1 to 3μm and the level of clustering was found to be reduced for the composites produced with higher number of passes and nano-particles were uniformly dispersed after four FSP passes. Moreover, Dadashpour et al. [29] fabricated AZ91/SiO_2 by FSP and found that reinforcing particles were distributed uniformly inside the base metal matrix without any formation of defect. Also, clustering of nanoparticles was observed at low FSP passes, which was resolved by increasing no. of FSP passes. This results in increase of strength of material.

Further, Navazania and Dehghani [30] fabricated AZ31/ZrO_2 nanopowders by FSP and found that increase in the passes of the FSP led to finer grains as well as less agglomeration of the ZrO_2 particles, thus enhancing the pinning effect of particles. This pinning effect retards the grain growth which leads to improvement of mechanical properties such as strength and hardness.

Navazania and Dehghani [31] also fabricated 5µm TiC particles on the surface of AZ31 magnesium alloy and found that by adding TiC particles; average grain size was reduced from 40µm to 12µm. Also, TiC particles had pinning effect on Grain Boundaries which restricted grain boundary movement and therefore grain growth was reduced. Intense temperature and severe plastic deformation resulted in fine microstructure. Also, discontinuous dynamic recrystallization was the main mechanism involved in refinement of microstructure. Average hardness was increased from 50Hv to 79Hv after adding reinforcement. Recently, Balakrishnan et al. [32] synthesized TiC/AZ31 surface composites using FSP. There was uniform distribution of TiC particles without any formation of clusters. Moreover, there was no interfacial reaction between the Mg matrix and TiC particles due to insufficient temperature developed in the matrix which can initiate the reaction.

Jiang et al. [33] successfully fabricated nano-SiO_2 particles into the AZ31 Mg alloy matrix by FSP. The authors reported that distribution of SiO_2 particles resulted grain refinement of equiaxed ultrafine grains with sizes of less than 1 µm. Moreover, hardness of the SiO_2/AZ31 composites was found to be 90 Hv which was nearly two times than that of the original alloy. This increase in hardness was attributed to dispersion of high strength SiO_2 particles and grain refinement taking place in the stir region of AZ31/SiO_2 composites.

In the work of Lee et al. [28], it was observed that the nano-SiO_2 particles remained as amorphous and not transformed to a crystalline phase during FSP. This was due to the lower temperature processing conditions in FSP which indicates heat that has been generated during the process was insufficient to initiate transformation in SiO_2 particles. Another significant observation from the TEM studies was the presence of MgO and Mg_2Si particles in the matrix. The authors suggested that these phases were formed during FSP due to the reaction of SiO_2 and Mg at the processing temperatures. The presence of these phases was also confirmed by the XRD method. Hardness was observed to increase up to two times for the composite compared with that of the parent AZ61 alloy.

Asadi et al. [34] fabricated AZ91/SiC surface nanocomposite layer by 8 FSP passes with the help of groove filling and covering method. From a starting grain size of 150 µm, grain refinement was achieved up to 600 nm and 7.21 µm in AZ91/SiC composite and FSPed AZ91 without SiC particles, respectively. It was a clear observation that the increase in the tool rpm influenced the microstructure evolution due to the generation of higher amounts of heat, which led to grain growth and also decreased the surface hardness. But increase in the

tool traverse speed resulted in lower grain size and higher hardness. Microhardness increased from 63 Hv to 115 Hv and 90 Hv for the composite and AZ91 without SiC particles, respectively, after eight FSP passes. A higher level of uniformity in the distribution of SiC was achieved by changing the tool rotating direction. In a similar work by Khayyamin et al. [35], FSP was done to fabricate AZ91/SiO_2 surface composites at three different traverse speeds (20, 40, 63 mm/min) and a fixed rpm of 1250. It was revealed that with increase in tool travel speed, grain size reduced which ultimately increased the hardness. Therefore, it is evident from the following discussion that higher tool travel speeds decrease the localized heat and reduce the grain growth issue during FSP.

Some of the studies also mentioned about the optimum traverse speed which will produce the sound and defect free processed zone. Similar to the work of Asadi et al. [34], Erfan and Kashani-Bozorg [36] observed the influence of tool rpm and tool traverse speed on the distribution of nano-sized SiC particles in AZ31 magnesium alloy. It was reported that as tool rpm increases, the level of clustering of SiC particles was found to be reduced. Also, the grain size was reduced with the increase in tool traverse speed due to the less generation of heat. Another important observation from the work is the development of tunneling defect with higher traverse speeds. Therefore, it is clear from the above studies that there should be an optimum traverse speed which can achieve grain size reduction along with the sound and defect free stir zone.

Most of the above mentioned literature review is concerned with grain refinement, microhardness improvement, pinning effect of particles. Some of the research is also done on the improvement of mechanical properties such as UTS and elongation. Sun et al. [37] synthesized high strength AZ63/SiCp nano-composite using FSP. In their study, 5 FSP passes was done to fabricate the 40nm SiC particles on AZ63 magnesium alloy. Moreover, SiC particles were ultrasonically dispersed in ethanol before filling into groove to avoid clustering of nanoparticles. Some of the conclusions were:

- Base metal containing irregular coarse second phase intermetallic compound $Al_{12}Mg_{17}$ get dissoluted after 5 pass FSP. Only two phases occurred in the in SiC-AZ63 composite which clearly states that no interfacial reaction occurred between the base material and reinforced particles during FSP.
- Vicker hardness was found to be increased from 80 Hv to 109 Hv. Further, UTS was found increased from 160 Mpa to 312 MPa.

- The strengthening mechanism of composites was explained by the pinning effect of particles at grain boundaries and the particles present inside the grain which prevent the dislocation slipping as shown in fig.4. This was explained like, as the tensile stress is increasing, the dislocation inside the grain began to slip. The existence of nanoparticles can stop the dislocation slipping. The dislocation line would form a dislocation loop around the nanoparticles, which increase the dislocation density, so the material would need more stress to deform.

FSP parameters like traverse speed, pin profile, rotational speed, tool tilt angle and Penetration Depth play role in the modification of microstructure and defect formation. Asadi et al. [38] fabricated 5μm SiC/AZ91 surface composite by FSP and studied the effect of process parameter, Penetration Depth (PD). There is an optimum penetration depth which results in formation of defect free FSPed specimen. At high PD, sliding mode of friction changes to sticking mode of friction which results in sticking of base metal to the tool. But at low PD, a longitudinal crack develops in the processing zone which results in tunneling type of defects in the stirred zone. Optimum PD depends on tool tilt angle and rotational speed like, increasing rotational speed and decreasing tilt result in decrease of PD. Optimum PD for 3.5°, 3° and 2.5° tilt angle were 0.40, 0.30 and 0.22 mm, respectively, when the rotational and traverse speeds were 1120 rpm and 63 mm/min, respectively. Also, there is an opposite effect of traverse speed and rotational speed on grain growth. Increase of traverse speed leads to decrease in grain size while increase of rotational speed leads to an increase in grain size. Therefore, by adding SiC particles, grain structure is refined from 150 to 7.17 μm and microhardness is increased from 63 to 96 Hv.

Azizieh et al. [39] studied the effect of rotational speed, pin profile, no. of FSP passes and particle size on the AZ31/Al_2O_3 nano-composite fabricated by FSP. Firstly, the authors discovered that the threaded profile tool was best among the non threaded profile tool and three flute profile tool, since threaded profile fabricated the composites without any cavity formation and with better particle distribution unlike the tunnelling defect and tool jamming shown by three flute profile while poor particle distribution shown by non threaded profile. All further investigations were done on threaded profile produced composites. Secondly, the authors investigated the combined effect of rpm and no. of FSP passes on the particle distribution, grain size and microhardness of the composite fabricated by threaded profile tool. Results revealed that with increase in rpm from 800 to 1200, the average grain size of the composite was increased due to the higher heat input while with increase in no. of FSP

passes from 2 to 4; average grain size was reduced at a fixed rpm. Moreover, with increase in rpm and no. of passes, the clustering of nanoparticles reduces i.e. better particle distribution due to higher heat input and more material flow in the stir zone. One of the important finding from this study was that at higher rpm of 1200, even the finely distributed Al_2O_3 particles were not able to retard the grain growth in the stir zone due to the combined effect of shattering or fragmentation of matrix grains and alumina particles, and grain growth by heat generation. Due to these effects, composites fabricated at higher rpm of 1200 shows less microhardness value (86 Hv at 4 passes) compared to the composites (92 Hv at 4 passes) processed at lower rpm of 800. At last, authors studied the effect of particles size ranging from no particle addition to micro particle (0.35 μm and 1 μm) and ultimately to nanoparticles (35 nm) on grain size and microhardness of the composite. Results exhibited that grain size was effectively refined in case of nanocomposite compared to composite with micro-particles, FSPed sample without particles addition and initial state of matrix. Also, with decrease in particle size the hardness value increases i.e. the nanocomposite had the highest hardness value of 90Hv in the stir zone compared to other studied particles. This is due to higher distribution of nanoparticles which ultimately lead to severe pinning effect at the grain boundary of the matrix.

Some studies also presented the rotational speed and traverse speed ratio (ω/ν) as a FSP parameter. Faraji and Asadi [40] synthesized AZ91 with Al_2O_3 nanoparticles (30 nm) by FSP and studied the effect of rotational speed/traverse speed ratio (ω/ν), FSP tool pin profile and no. of passes on the microstructure and microhardness of the produced nanocomposite. Initially, with the square profile and circular profile FSP tool pin, authors fabricated the composite at a rotational speed of 900 rpm and traverse speed of 40 mm/min and obtained that it was difficult to achieve uniform distribution of particles even in low traverse speed in the case of circular profile tool. This is due to the absence of pulsating stirring action in case of circular profile tool as this action intensifies the mixing of particles in the matrix. All further investigations were carried out using square profile FSP tool. It was revealed that higher ω/ν ratio leads to better distribution of Al_2O_3 nanoparticles i.e. less accumulation of alumina particles and consequently smaller grain size of the composite layer. Thus, optimum conditions for producing the sound surface layer were achieved by square tool and rotational speed of 900 rpm and traverse speed of 40 mm/min. Moreover, microhardness was also increased at higher ω/ν ratio due to the small grain size which was justified by Hall-Petch relationship. It was also reported that increase in number of passes results in increase in

microhardness; since more passes homogenizes the particles distribution, decreases the alumina agglomeration and consequently decreases the grain size. Also, lower travel speeds led to form thick TMAZ due to the more heat generation compared with higher travel speeds.

2.4.2.2 Effect of FSP on wear resistance of Magnesium composites

FSP is found to be an effective technique for the enhancement of wear properties by incorporating secondary phase particles into the magnesium matrix. Lu et al [41] presented the independent and hybrid effect of n-Al_2O_3 and CNTs on the wear resistance of AZ31 Mg alloy. Firstly, all composites independent and hybrid were found more wear resistance than base AZ31 alloy. Secondly, individual n-Al_2O_3 reinforcement particles wear was lower than that of independent CNTs; however, former friction coefficient was higher. Finally, wear and friction coefficient of the composite having 0.1%$A1_2O_3$ and 0.2%CNTs was lower than those of other composites when the load was higher than 1.95 MPa while wear and friction coefficient of the composite having 0.2%$A1_2O_3$ and 0.1%CNTs was lower than others when the load was less than 1.30 MPa. Author tells the hybrid effect was due to the hardening and lubrication effect provided by n-$A1_2O_3$, and CNTs respectively.

Reddy et al [42] introduced silicon carbide (SiC) and boron carbide (B_4C) particles into the surface of ZM21 magnesium alloy by holes filling and closing method using FSP. Some of the findings were that there is significant improvement in the hardness of FSPed alloy with particles of B_4C and SiC. Also, FSPed B_4C reinforced magnesium alloy exhibited relatively higher hardness compared to SiC reinforced because of higher hardness of B_4C. This result in less wear rate (friction coefficient average 0.025) revealed by B_4C particle reinforcement compared to base metal (friction coefficient average 0.2).

Faraji and Asadi [40] also studied the wear characteristics of the AZ91 alloy reinforced by Al_2O_3 nano particles. Result shows that addition of nano-sized alumina particles decreased the volumetric wear rate from 0.0175mm^3/Nm to 0.0025mm^3/Nm, almost 7 times. Author investigated the root cause concerned with the increase of wear resistance and found that better distribution of alumina particles result in high hardness which ultimately leads to high wear resistance. Also, the presence of alumina particles decreases the direct load between the specimen surface and counter disk which results in decrease of wear rate.

Chen et al. [43] produced a surface composite layer on thixoformed AZ91 magnesium alloy by reinforcing with SiC particles using FSP and examined the tribological properties. Grain

refinement from 120 to 3.1 μm takes place. The authors found that the distribution of SiC particles was uniform throughout the stir zone with slight agglomeration. It was suggested to carry out multi passes to reduce this agglomeration. Surface hardness and wear resistance were found to be increased for the surface composite compared with as received alloy. Coefficient of friction was also reduced for the composite compared with other samples. The prime reason behind the improved tribological properties of the composite was the presence of SiC particles at the surface, which strengthened the magnesium matrix and improved its wear resistance.

2.4.2.3 Recent development in FSP fabrication

All the above literature studied is concerned with the fabrication of composites by groove filling and closing method or hole filling and closing method. Another method of dispersing second phase particles in the Magnesium matrix is Sandwich method. In this method, a sandwich kind of arrangement is made by placing the reinforcement phase in the form of layer or laminate between the workpiece to be FSPed. Mertens et al. [44] dispersed carbon fibers in AZ31B alloy by sandwich method. It was observed that AZ31B sheets processed at two different tool traverse speeds (80 mm/min and 300 mm/min) with a higher rpm (1500) exhibited uniform distribution of the carbon fibers with defect free stir zone. Grain refinement was also influenced by the presence of carbon fibers. The composite exhibited smaller grain size (10.0 ± 3.6 μm) compared with FSPed AZ31 without carbon fibers (16.4 ± 5.4 μm), which can be attributed to the pinning effect of the reinforcing phase. This result was opposite compared to another work of Mertens et al. [45], in which carbon fibres were dispersed in AZ91D matrix by sandwich method. It was reported that inhomogeneous distribution of carbon fibres with porosity and defective stir zone was noticed for AZ91D magnesium alloy with the higher tool rotational speeds and travel speeds unlike in case of AZ31B alloy. Defect free composite of AZ91D alloy was produced at lower tool rotational and traverse speeds (500 rpm and 80 mm/min). The reason may be due to the existence of more amounts of hard and brittle $Mg_{17}Al_{12}$ intermetallic phase in the AZ91D magnesium alloy, which needs appropriate tool travel and rotational speeds to break and dissolve in the secondary phase.

One of the recent developments in field of FSP is the development of newly designed FSP tool named as direct friction stir processing (DFSP) tool. In DFSP tool FSP, reinforcement particles are not introduced into the surface of base metal (by making groove) before

processing as in case of normal FSP. Here, the particles are introduced when the processing is going on with the help of a hole designed within DFSP tool. Huang et al. [46] synthesized AZ31/SiC surface composite using this tool. Main findings were:

- Grain refinement was achieved in DFSPed composite up to 1.24 µm compared to FSPed AZ31 (5.21 µm) and from the as received AZ31 size of 16.57 µm.
- Fine and homogeneous distribution of reinforced particles was noticed at the surface of the composite produced by DFSP. The width of the particle distribution zone was found to be more in DFSP compared with that of FSP. More amount of reinforcement particles can be introduced into the matrix in a single pass compared to normal FSP method.
- Microhardness was nearly doubled for the composite fabricated by DFSP compared with as received condition. Composite fabricated by FSP has also shown increased hardness but inferior when compared with DFSPed composite.
- Initial machining processes such as producing grooves or holes to fill the secondary phase particles on the surface of the workpiece can be completely eliminated using DFSP tool which is an advantage that reduces the machining processes such as groove cutting or drilling the holes and increases the productivity however, there is a limitation observed by this tool is the penetration thickness. The thickness of surface composite layer produced by DFSP is relatively less compared with the surface composite produced by FSP.

2.4.3 Important findings from the literature

- FSP studies done on Mg alloys, mainly AZ series reveal that FSP resulted in remarkable grain refinement and significant breakup and dissolution of the coarse, network-like secondary eutectic phase β-$Mg_{17}Al_{12}$ distributed at the grain boundaries which results in improvement of mechanical properties. While, FSP of Mg alloys containing RE elements results in dissolution of $Mg_{12}Nd$ intermetallic phase in Mg matrix.
- Machine parameters considered during FSP are tool travel speed, rotational speed, tilt angle and penetration depth. Out of these, tool travel speed and rotational speed have major effect during FSP. Penetration depth and tilt angle are also considered variable as shown by Asadi et al. [38].

- Mostly in all the above mentioned studies of surface composites, reinforcement particles were introduced in the magnesium matrix by groove filling and closing method.
- From the above review, it is observed that in fabrication of surface composites, tool traverse speed and rotational speed have both good and bad effects.
- Increase in tool rotational speed leads to increase in grain size which decreases the microhardness due to the more heat input but higher rpm leads to homogeneous distribution and breaking up of clusters as shown by Azizieh et al [39].
- Moreover, higher rpm accelerates the pinning effect of particles at the grain boundary which retard the grain growth and thus increasing strength and hardness as shown by Navazania and Dehghani [31]. But in the work of Azizieh et al [39], even the finely distributed Al_2O_3 particles were not able to retard the grain growth due to the combined effect of shattering of matrix grains and alumina particles, and grain growth by heat generation.
- While increase in traverse speed leads to decrease in grain size and grain refinement which ultimately results in increase of hardness due to less local heat input as shown by Khayyamin et al [35].
- Number of FSP passes also effects the fabrication of surface composite by reducing the agglomeration of particles. Multi-pass FSP leads to a reduction in size of cluster and uniform distribution of reinforcement particles and thus decreases the grain size of matrix as depicted by Lee et al. [28]
- Tool parameters like direction of tool rotation (reported by Asadi et al. [34]), tool tilt angle (Asadi et al. [38]), and tool geometry such as probe shape (Faraji and Asadi [40] and size (Azizieh et al. [39]) have considerable effect during FSP.
- Also, there are recent developments in FSP such as DFSP method and sandwich method of reinforcement introduction into the magnesium matrix.

2.5 Literature Gap

- Most of the research conducted on FSP focuses on aluminum alloys. Despite the potential weight reduction that can be achieved using magnesium alloys, limited study is done on FSP of magnesium alloys.
- Further, most of the studies done on magnesium alloys is restricted to AZ series such as AZ31, AZ91, AZ63, AZ61 and somewhere ZM21 alloy. There is limited investigation done on Mg alloys containing Rare Earth (RE) elements while no work is carried out on fabrication of RE element based Mg alloy surface composites.
- Moreover, there is no study on the Mg alloy having composition Mg-4Al-3Zn-3Sn-3Pb-0.5MM. Misch metal has a major advantage over Rare Earth elements since use of RE elements to improve the elevated temperatures of Mg alloys is not economical due to its high cost and difficulties in achieving in homogeneous structure. The use of MM is more economical since cost of MM is 10 times cheaper than individual RE elements.
- Secondly, reinforcement particles used for composite fabrication are limited to Al_2O_3, SiC, TiC etc. There is almost no study in the FSP assisted fabrication of Mg alloy based composite having Boron Carbide (B_4C) as a reinforcement particle.
- At last, there is limited study on wear behavior of surface composites since most of the investigations are focused on grain refinement and mechanical properties such as microhardness.

CHAPTER-3

EXPERIMENTAL PROCEDURE

3.1 Materials

In this study, the experimental set-ups used for the work are briefly described. Mg-Al-Zn-Sn-Pb based alloy plate (130 mm length and 80 mm width) is selected for the present study. The alloy is designated as **H1 alloy**. H1 alloy is selected from the conventional casting done by G Gaurav et al. [47]. Composition of the studied alloy is mentioned in table 3.1.

Table 3.1
Chemical Composition of the H1 alloy

Elements	Al	Zn	Sn	Pb	MM	Mg
% wt	4	3	3	3	0.5	Rest

where, MM= Misch Metal (Purity; 52%Ce-26%La-16%Nd-6%Pr)

The micron sized B_4C particles having an average particle size of 20 µm was selected as a reinforcement particle for fabrication of surface composites. The SEM micrograph of the particle is shown in Fig. 3.1.

3.2 Procedure

Friction Stir Processing (FSP) was performed with the help of indigenously developed FSW machine. For fabrication of surface composites, a groove of 1mm width and 4mm depth was made on another portion of H1 alloy plate with the help of milling machine. After this, groove was properly cleaned with acetone and Boron Carbide (B_4C) particles were introduced into the Magnesium matrix by groove filling and closing method. In this method, first of all groove was filled with B_4C particles and then groove was closed with the help of a probe less tool to prevent escaping of micro particles. At last, plate was subjected with an FSP tool as shown in fig. 3.2 to produce Mg/B_4C surface composite. For every pass, the specimen was allowed to be cooled to the room temperature and all the experiments were carried out at room temperature. One portion of H1 alloy plate was also subjected to simple FSP without the addition of B_4C particle. The FSP procedure to produce the surface

composite is schematically shown in Fig. 3.3. For better study, H1 alloy condition is designated as shown in table 3.2

Table 3.2

Designation of H1 alloy condition

H1 Alloy Condition	Designation
Base metal	BM
FSPed without B_4C	H1/FSPed
FSPed with B_4C	H1/B_4C

Processed zone during FSP is shown in figure 3.4. The specimen was clamped on the hydraulic fixture with mild steel backing plate. Further, surface appearance of the FSPed plate without particle is shown in figure 3.5.

3.2.1 Process Parameters

Based on the literature review and number of trials performed, by keeping one parameter fixed and others varied, following parameters were fixed during FSP to obtain the surface composite without any formation of defects:

- Constant Rotational Speed of 1000 rpm.
- Constant Traverse Speed of 50 mm/min.
- Tilt angle of 0º.
- Number of FSP passes done are 3.
- Plunge depth of 0.15 mm.
- Groove of 1mm width and 4mm depth.

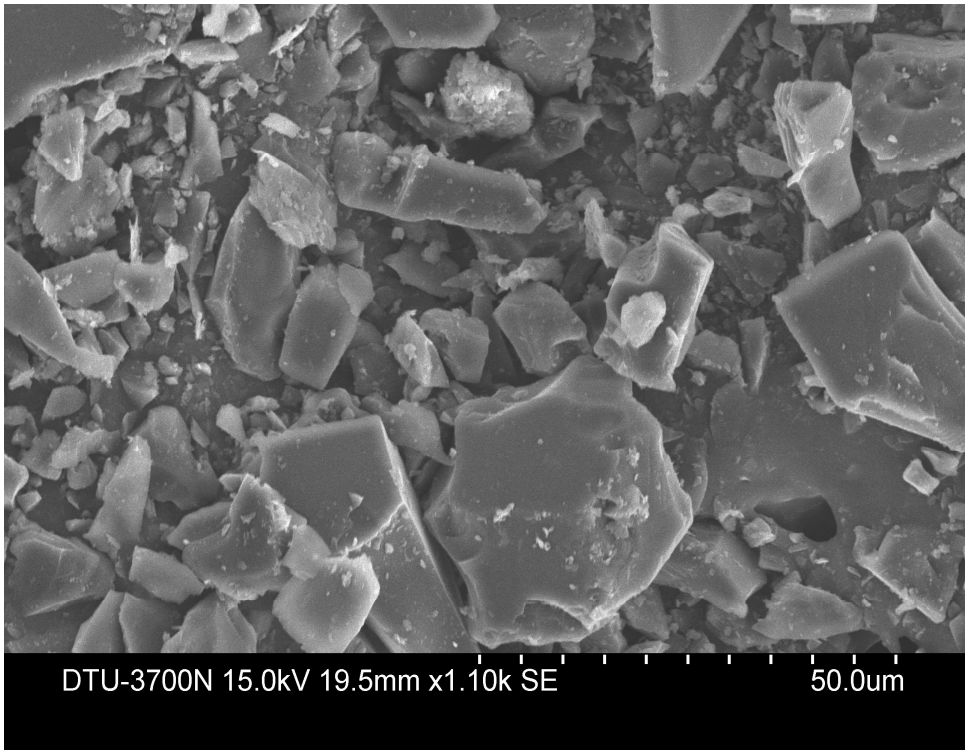

Figure 3.1 SEM micrographs of as-received B_4C micro particles.

Figure 3.2 A simple FSP tool.

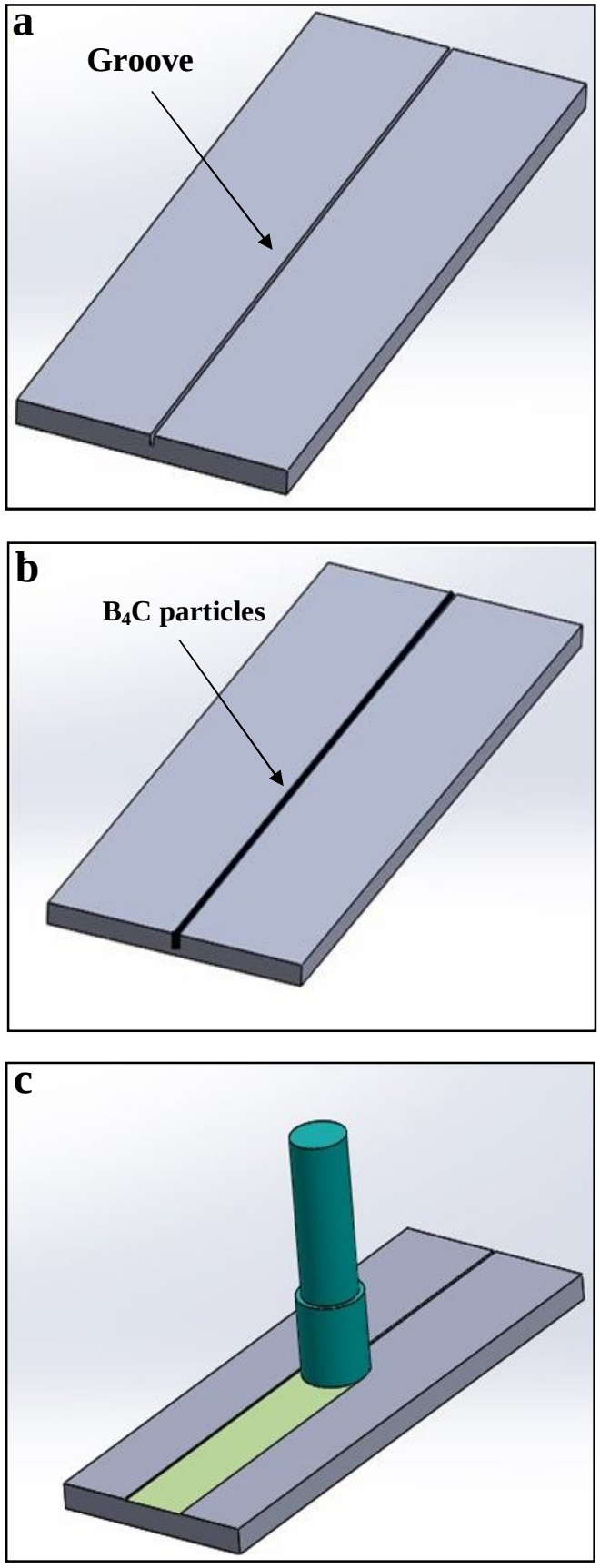

Figure 3.3 FSP procedure for surface composite fabrication: (a) Groove Cutting; (b) Compacting Groove with B_4C particles; (c) FSP performed with a square pin FSP tool.

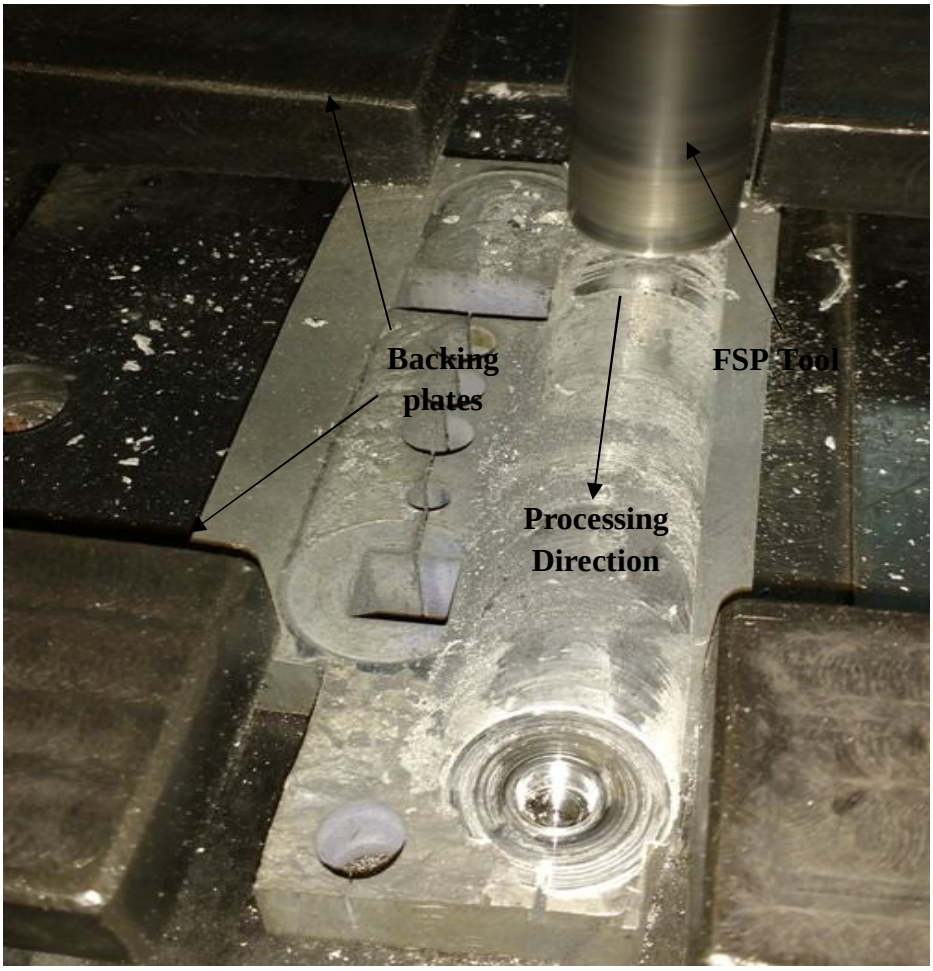

Figure 3.4 Friction Stir Processed Zone.

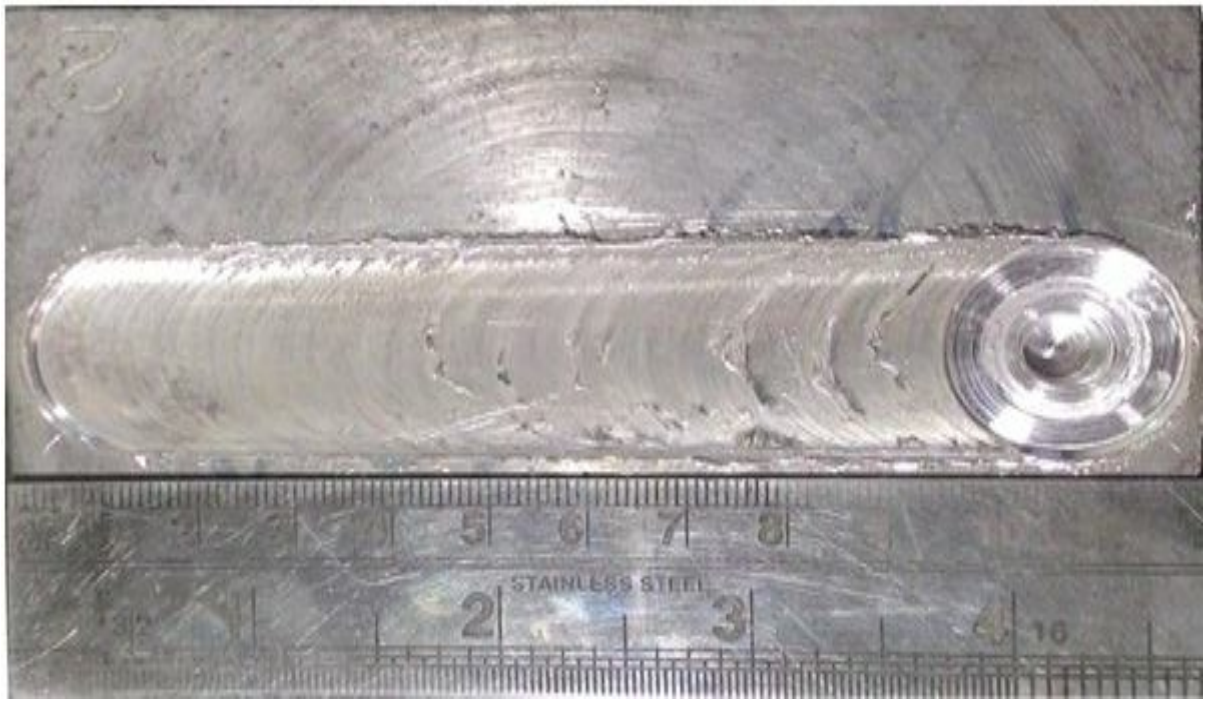

Figure 3.5 Surface appearance of FSPed H1 alloy plate without B_4C.

3.2.2 FSW Machine

An indigenous developed friction stir welding machine (R V machine tools, FSW-4T-HYD, shown in figure 3.6) was used for Friction Stir Processing. Specifications of the machine are as follows:

- Power – 11 KW
- Rpm – 3000
- Load capacity – 25 KN
- Clamps – hydraulic actuated
- Backing plate groove – 200 mm × 80 mm

3.2.3 FSP Tool Specifications

Tool used during FSP (shown in fig.3.7) has following specifications:

- Shoulder diameter of 24 mm.
- H-13 tool steel hardened to 55 HRC
- Pin profile is of square.
- Pin size of 8 mm diagonally.
- Pin length is 5 mm.

3.2.4 Volume fraction calculation

Volume fraction of boron carbide (B_4C) particles used during FSP was calculated from the following expressions given below:

$$\text{Volume Fraction} = \frac{\text{Area of Groove}}{\text{Projected Area of Tool Pin}} \times 100$$

where, Area of Groove = Groove width × Groove depth

Projected Area of Tool Pin = Pin Size × Pin length

From the above expressions, volume fraction of B_4C particles comes out to be nearly 13%.

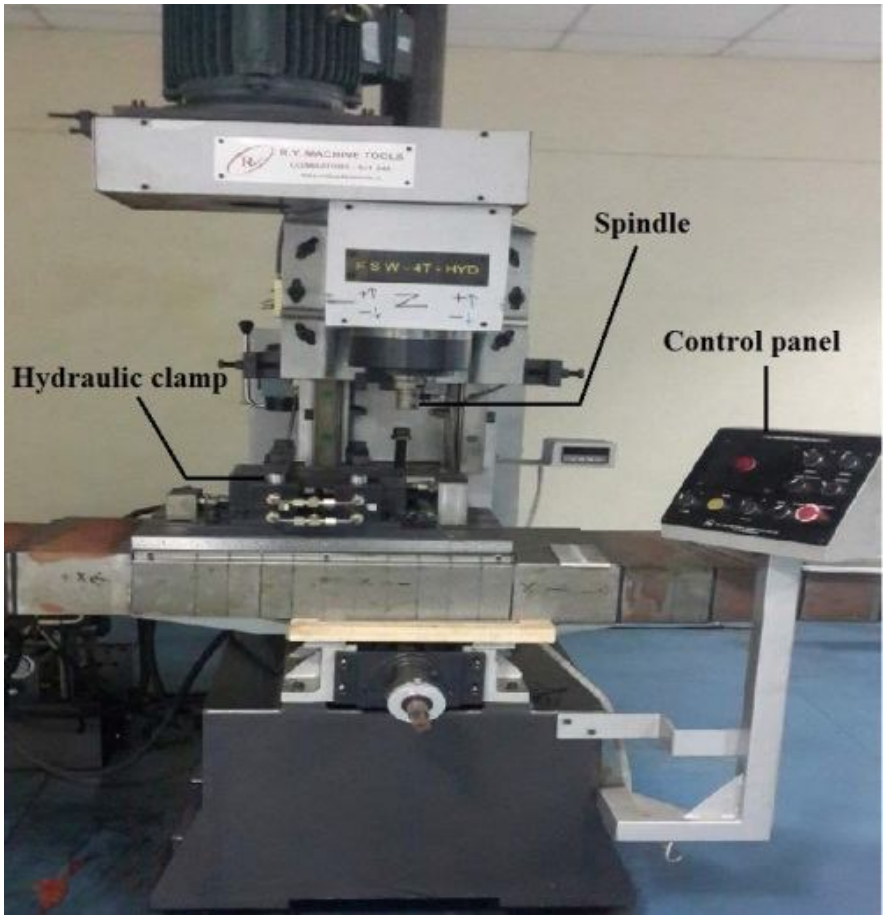

Figure 3.6 Friction Stir Welding Machine.

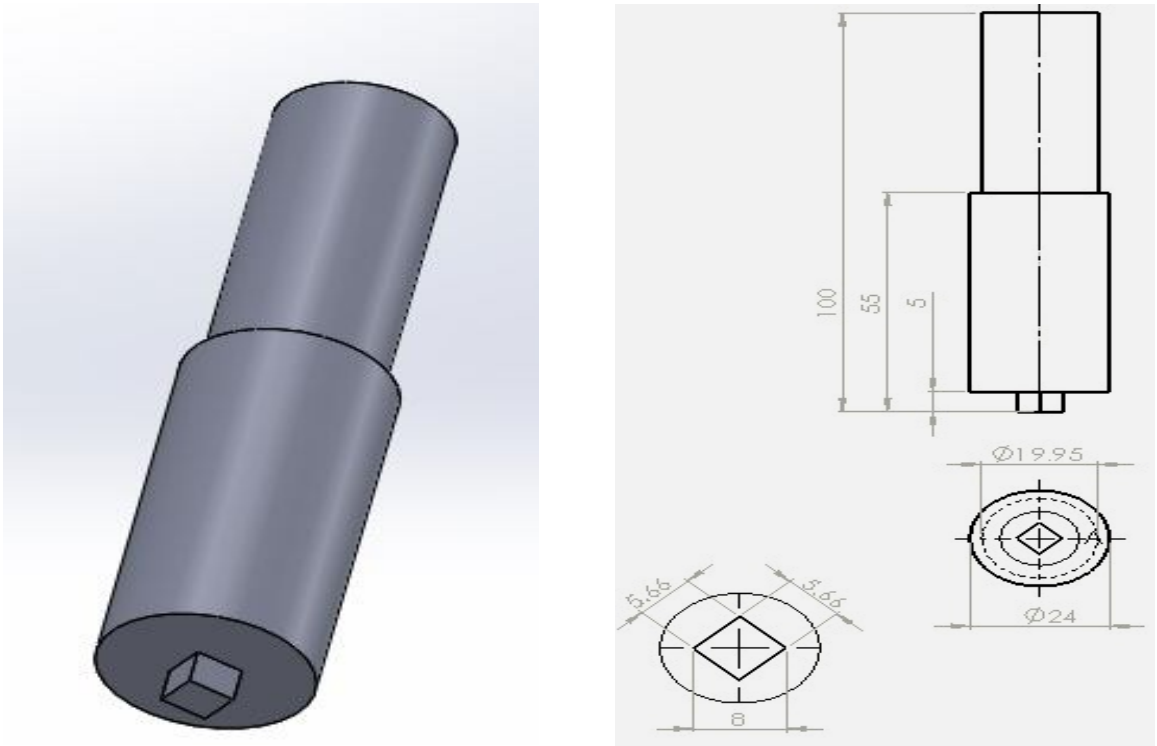

Figure 3.7 Schematic illustration of FSP tool.

3.3 Sample Preparation

To study microstructure, microhardness and wear; samples were cut in transverse direction from the middle portion of stirred zone of the FSPed surface (with and without B_4C) with the help of wire EDM as shown in figure 3.8. Two non circular samples each from H1/FSPed and H1/B_4C processed surface having size 10 mm and 10×20 mm were cut for microstructure observation and microhardness study. Moreover, two circular samples each from H1/FSPed and H1/B_4C processed surface having 8 mm diameter were taken for wear test. In the same way samples were also taken from the base metal H1.

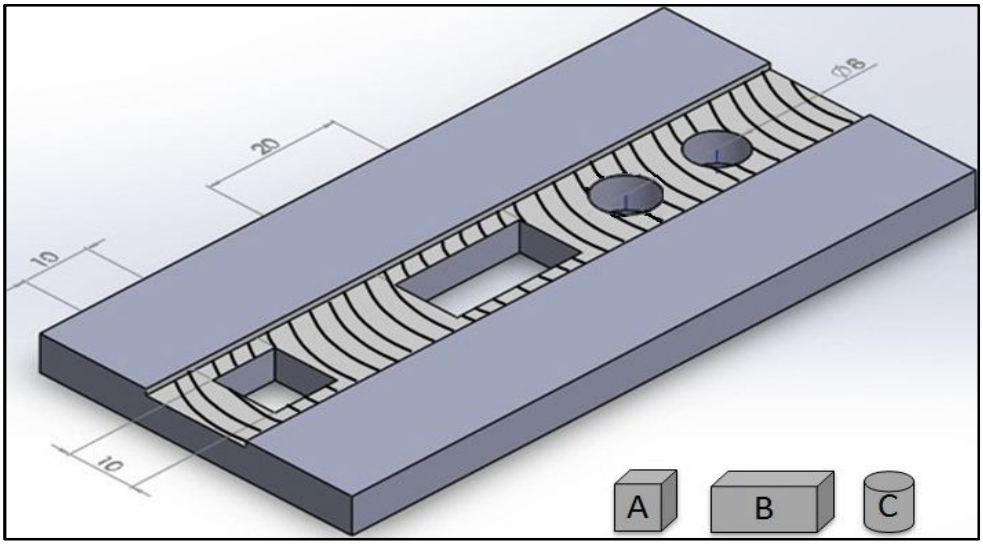

Figure 3.8 Samples cut for investigation: (A) Microstructure (B) Microhardness and (C) Wear behavior

3.4 Microstructural Observation

Figure 3.8 shows the samples cut from the stirred zone for microstructure study. This section consists of Polishing, Etching, Optical Microscopy (OM) investigation, Scanning Electron Microscopy (SEM) study, Energy Dispersive Analysis of X-ray Spectroscopy (EDAX) and X-ray Diffraction (XRD) study.

3.4.1 Polishing

Before doing polishing operation, samples were mounted with the help of resin and hardener as shown in figure 3.9. Mounting was done for easy holding of the samples, as the samples were small and cannot be hold during polishing resulting in uneven and improper polishing. Now, the mounted samples were dry polished using different grades of emery paper with

progressively coarser to finer one (100, 120, 220, 320, 400, 600, 1200, 2000 grits) in the metallurgical laboratory.

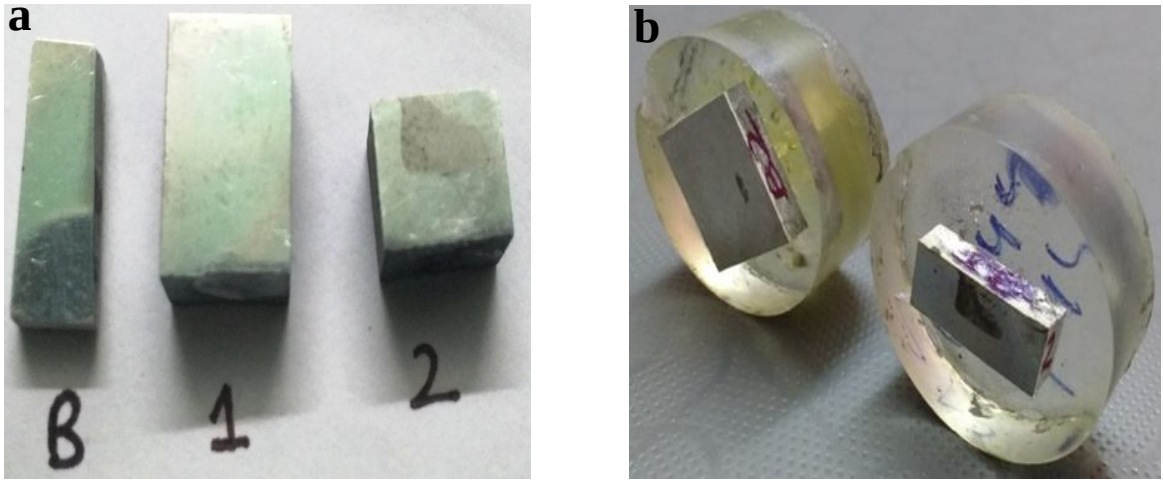

Figure 3.9 Figure representing (a) Microstructure Samples (b) Mounting of Samples

After performing dry polishing, initially wet polishing was done by making the samples contact against the rotating disc having fine grit emery paper as shown in figure 3.10. Finally, wet polishing was done in a rotating disc of proprietary cloth (velvet type) with the application of alumina powder having grade I, II and III as shown in figure 3.10. Intermittent drying of samples was also done by the hand dryer provided in the machine. Since Mg is a soft material care was taken during polishing to avoid scratches and excessive surface contamination. Finally, the samples were cleaned using ethanol as cleaning with water was not sufficient to remove surface contaminants.

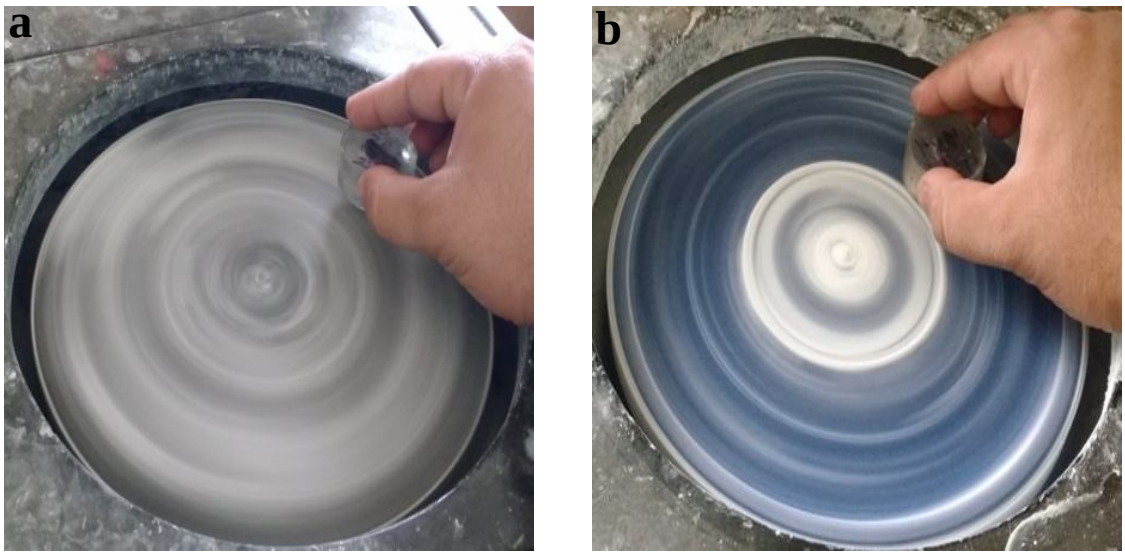

Figure 3.10 Wet Polishing by (a) Fine grit emery paper (b) Alumina Powder

3.4.2 Etching

To reveal the grain structure, samples were finally etched using a chemical solution of ethanol (100 ml), picric acid (6 g), acetic aid (5 ml) and water (10 ml) for 5-10 seconds. After chemical etching, a residual layer remained in the sample surface that was eliminated by immersion in ethanol.

3.4.3 Optical Microscopy (OM)

The microstructural evolution during the FSP were characterized using an Olympus Optical Microscope (OM), model GX 41 equipped with image analysis software, a camera having 10x, 20x, 50x and 100x lens and a computer. Indentations in the specimen which was developed during microhardness test were also visualized by OM. OM images were taken for all three H1 alloy types through 10x objective lens.

3.4.4 Scanning Electron Microscope (SEM)

Scanning electron microscope (SEM) (Hitachi S3700) was used to examine the distribution of the reinforcement particles (B_4C) in the H1 alloy. Worn out surfaces during wear testing of all three H1 alloy types were also analyzed using SEM to understand the wear mechanism.

3.4.5 X-ray diffraction (XRD)

XRD (BRUKER D8 ADVANCE) was done to confirm the presence of reinforcement particle in the magnesium matrix. XRD spectrums were obtained using powder diffractometer with Cu-K_α radiation (λ = 1.5418 Å). The samples were polished and cleaned before subjecting to diffraction studies.

3.5 Microhardness Test

The vicker's microhardness testing machine (Model- MVK-H1, Mitutoyo) having specification as hardness ranging from 20 Hv to 1500 Hv and load ranging from 10gm to 1000 gm was used for microhardness test. Before the hardness measurement, samples were polished upto 1200 grit fine emery paper to remove the oxide and other scales for clear observation of indentation mark. The Vickers micro hardness values of the FSPed regions was measured along the processing direction (along the depth of specimen) using a load of 50 g with dwell time of 10 s. Six readings were taken for each FSPed sample (H1/FSPed and H1/B_4C) and its average has been reported as the hardness value of that particular sample.

3.6 Wear Test

3.6.1 Wear Sample Preparation

Wear samples of 8 mm diameter, which were cut from the stirred zone as discussed above, were small in size and difficult to hold in the wear testing machine. Therefore for easy holding, mild steel pins of 8 mm diameter were used as a dummy as shown in figure 3.11. These dummy pins were mounted on the wear samples as shown in figure 3.11. Mounting was done by drilling a hole of 2 mm diameter and 4 mm deep in the sample with the help of drilling machine; after that sticking of dummy pin to the processed wear samples was done with the help of Araldite and ultimately samples were kept drying for about 24 hours. Finally, filing was done on the flat surface of wear samples to avoid unevenness during wear test. In this way, total 5 wear samples were prepared for wear testing operation.

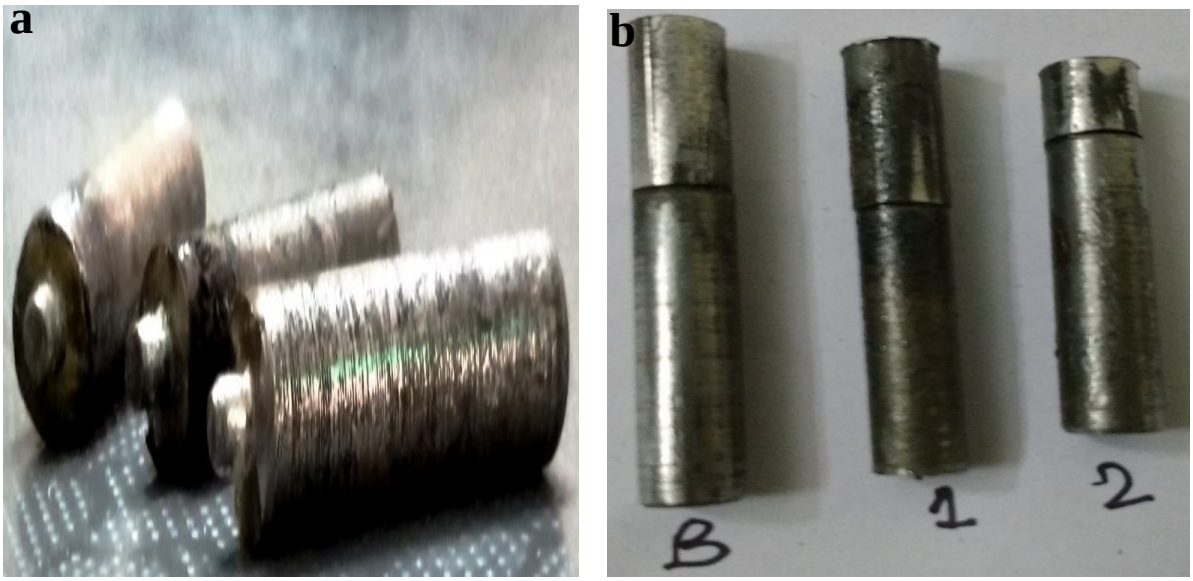

Figure 3.11 Figure representing (a) Mild Steel Dummy pins (b) Mounting of Wear Samples

3.6.2 Wear Testing Operation

The sliding wear test was carried out using pin-on-disc tribometer (model TR 20, manufactured by Ducom, Bangalore, India) in room temperature condition. Pins of 8 mm diameter were made to slide against the rotating counterdiscs of diameter 160 mm as shown in figure 3.12. The counterpart discs were made of EN-24 steel hardened to 52 HRC and the surface roughness (Ra) of 0.2 µm. Before the test, the surface of each pin was polished on 1200 grit emery paper. A constant track diameter of 100 mm and a constant sliding velocity of 1.5 m /s, which resulted in 286 rpm, were used in all 5 wear sample testing. Moreover,

sliding distance of 3000 m was fixed in all tests which give the 2000 seconds duration of each wear test. For every wear test, sample was cleaned with acetone and weighed to an accuracy of 0.001 mg by electronic weighing balance before and after wear test. Load was fixed for 30 N for base sample (B), FSPed sample without (1) and with particle (2). Similarly, load of 10 N was fixed for '1' and '2' type samples. Sensor output in the machine measured the frictional force in N and cumulative wear loss in mm as a function of time. Wear rate in mg/m was calculated from weight loss during wear. The friction coefficient between the pin specimen and disc was determined by calculating the ratio of frictional force (obtained from sensor output) and normal load (30 N or 10 N). All the worn sample surfaces were cleaned by acetone and examined under SEM.

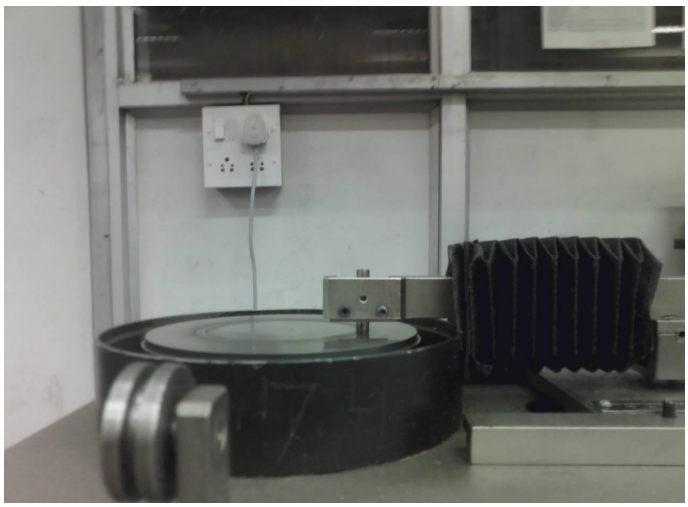

Figure 3.12 Pin-on-disc Tribometer.

3.6.3 Pin on Disk Tribometer Specifications

The specification of the machine is as follows:

- Pin diameter of 3, 4, 6, 8, 10 and 12 mm.
- Disc size of 165 mm diameter and 8 mm thickness.
- Disc speed ranging from 200 to 2000 rpm, infinitely variable in steps of 1 rpm.
- Disc material of EN-31 hardened to 62HRc.
- Normal load ranging from 1 N to 200 N in steps of 5 N.
- Frictional force ranging from 0 to 200 N.
- Wear track ranging from minimum diameter of 50 mm to maximum diameter of 100 mm.
- Sliding speed ranging from minimum of 0.5 m/s to maximum of 10 m/s.

CHAPTER-4

RESULTS AND DISCUSSIONS

This chapter deals with the effect of FSP on the microstructure, microhardness and wear properties of H1 alloy and Boron Carbide (B_4C) surface composite fabricated by Friction Stir Processing (FSP).

4.1 Microstructure Characterization

FSP resulted in successful fabrication of Mg alloy/B_4C surface composite. Fig 4.1 represents the microstructural images of the stirred zone (SZ) of all three H1 alloy types which was examined by optical microscope. After FSP, the microstructure of the SZ of without particle FSP is characterized by fine and equiaxed α-Mg grains. The primitive grains in SZ experience severe plastic deformation and dynamic recovery, while the coarse grains are broken. Therefore, this indicates that complete dynamic recrystallization (DRX) occurs during FSP but the time is too short for DRXed grains to grow up, leading to significant grain refinement. Further, with particle FSP is characterized by uniform distribution of reinforcement particles. Also, FSP leads to dissolution and breaking of secondary phase intermetallic compounds like MgZn, Mg_2Sn and Mg_2Al_3 (as reported by Gaurav et al. [47]) that were present in the base metal. Therefore, it can be concluded that FSP leads to uniform distribution of reinforcement particles and significant grain refinement of H1 alloy.

Fig 4.2 represents the SEM images of the transverse cross-section of FSPed alloy with B_4C particle at different scales. Reinforcement particles can be seen uniformly distributed in the magnesium matrix. To confirm the presence of secondary phase particle (B_4C) in the Mg matrix, XRD was done on H1/B_4C alloy. Fig 4.3 represents the XRD pattern of H1/B_4C alloy. The clear and large peaks of α-magnesium and marginal peaks of B_4C appeared in the XRD pattern clearly indicates the presence of B_4C particles in the magnesium matrix. These reinforcement particles restrict the grain growth within the Mg matrix due to the pinning effect which ultimately results in decrease of grain size.

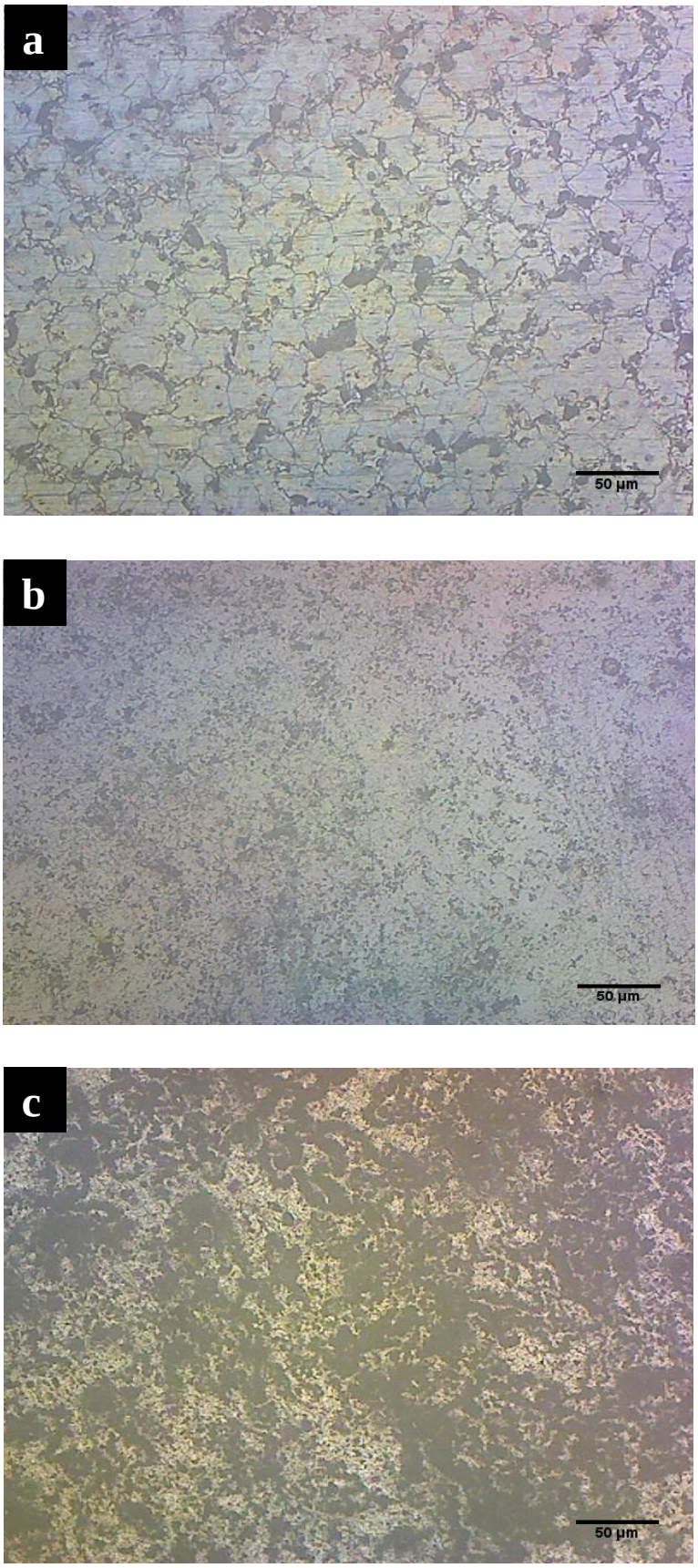

Figure 4.1 OM images of transverse cross-sectional of H1 alloy (a) Base Metal, (b) FSPed without B_4C micro sized particle and (c) FSPed with B_4C micro sized particle.

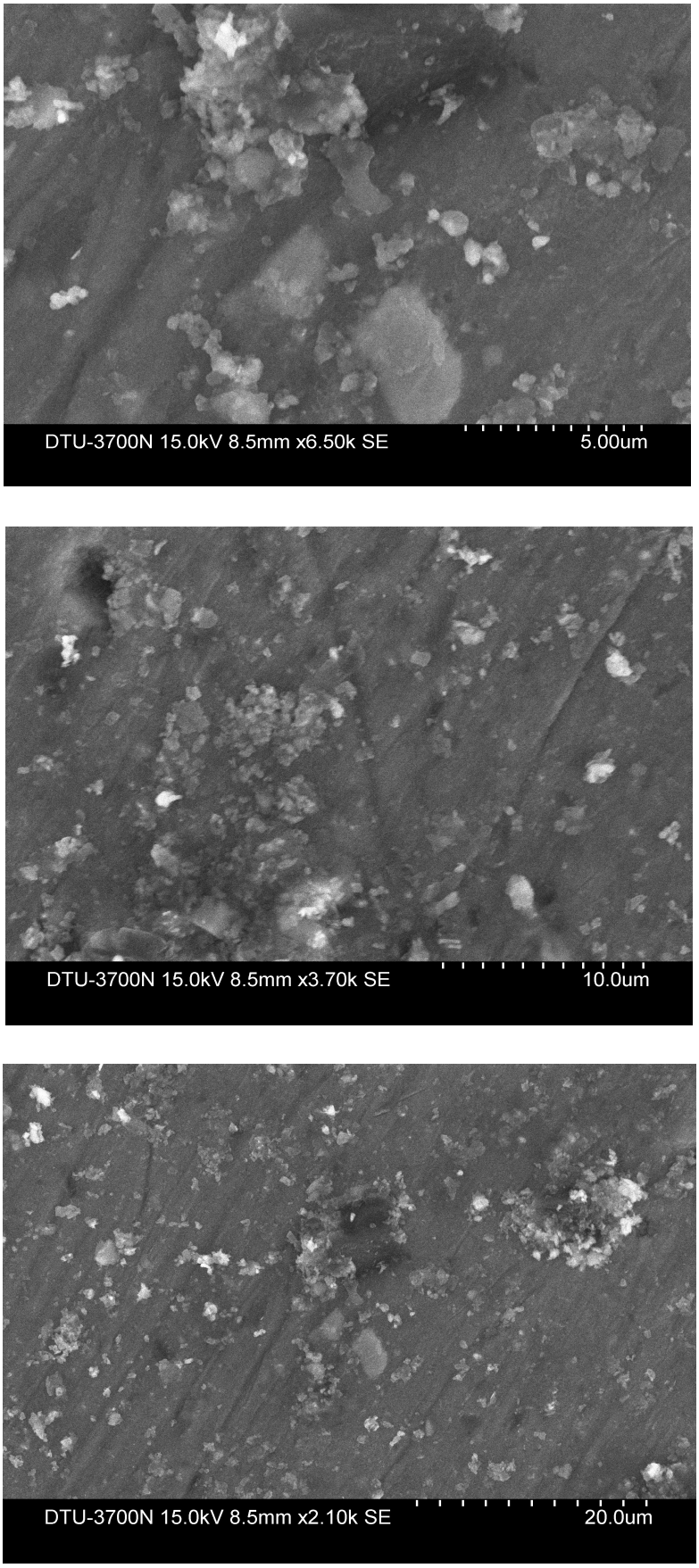

Figure 4.2 SEM micrographs of H1 alloy FSPed with B_4C micro sized particle.

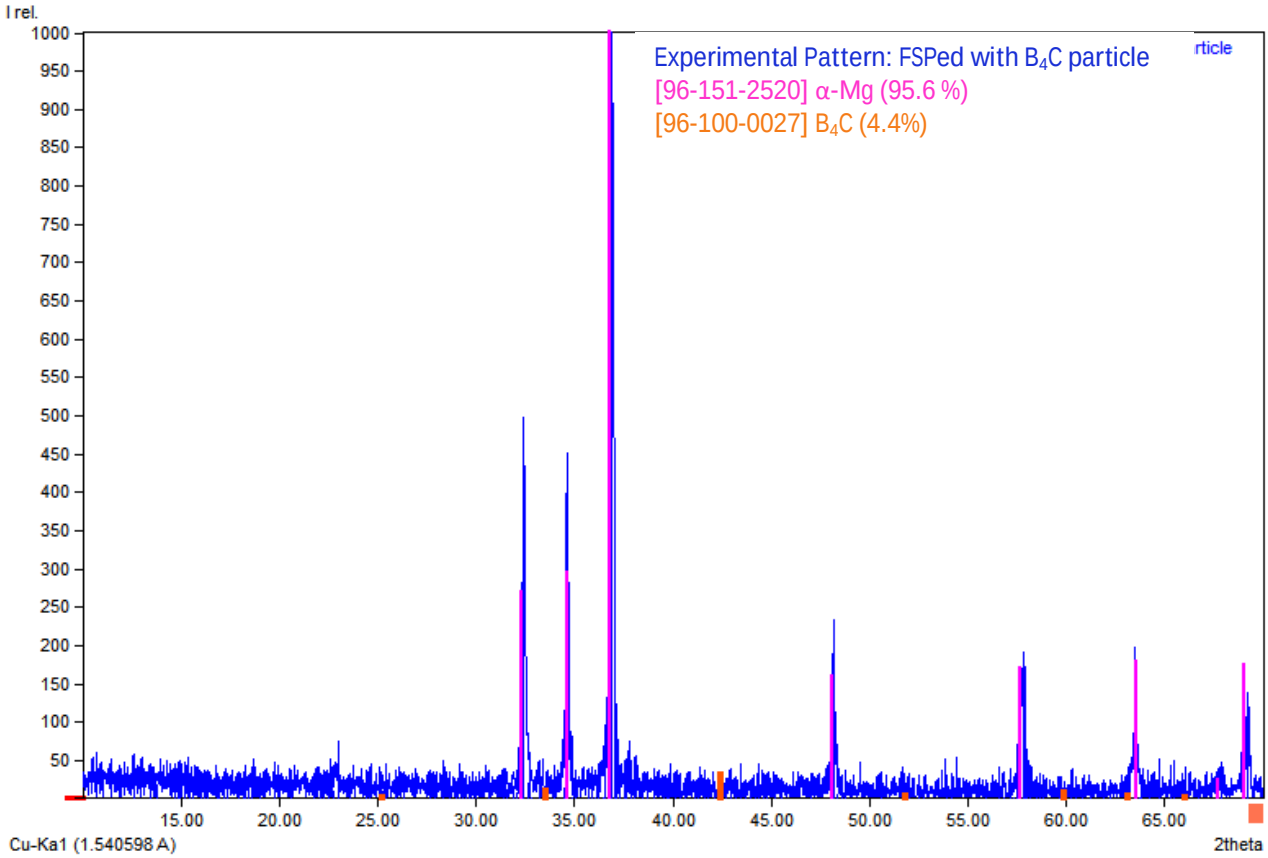

Figure 4.3 XRD pattern of H1 alloy FSPed with B_4C micro sized particle.

Fig 4.4 and 4.5 represents different regions formed during FSP in FSPed/H1 and H1/B_4C. There were three different and common regions identified after FSP in both alloy types:

- Transition region which connects SZ and TMAZ, since it is characterized by change of very fine region to less fine region.
- Thermo-mechanically affected zone (TMAZ) which was found in the close vicinity of SZ and is subjected to the thermal cycle and mechanical stress. Therefore, continuous dynamic recrystallization (CDRX) occurs in the part of the zone and fine equiaxial grains nucleate at the grain boundaries of original grains and grow up to some extent, hence mixed zone of coarse grains and fine grains appeared in the microstructure, as shown in Fig 4.4 and 4.5. The elongated unDRXed and finely equiaxial DRXed grain structures are characterized in the TMAZ.
- Heat Affected Zone (HAZ) which only experiences a thermal cycle but does not undergo any plastic deformation. Therefore, HAZ still retains the similar microstructure to BM and grain size is slightly larger than that of BM.

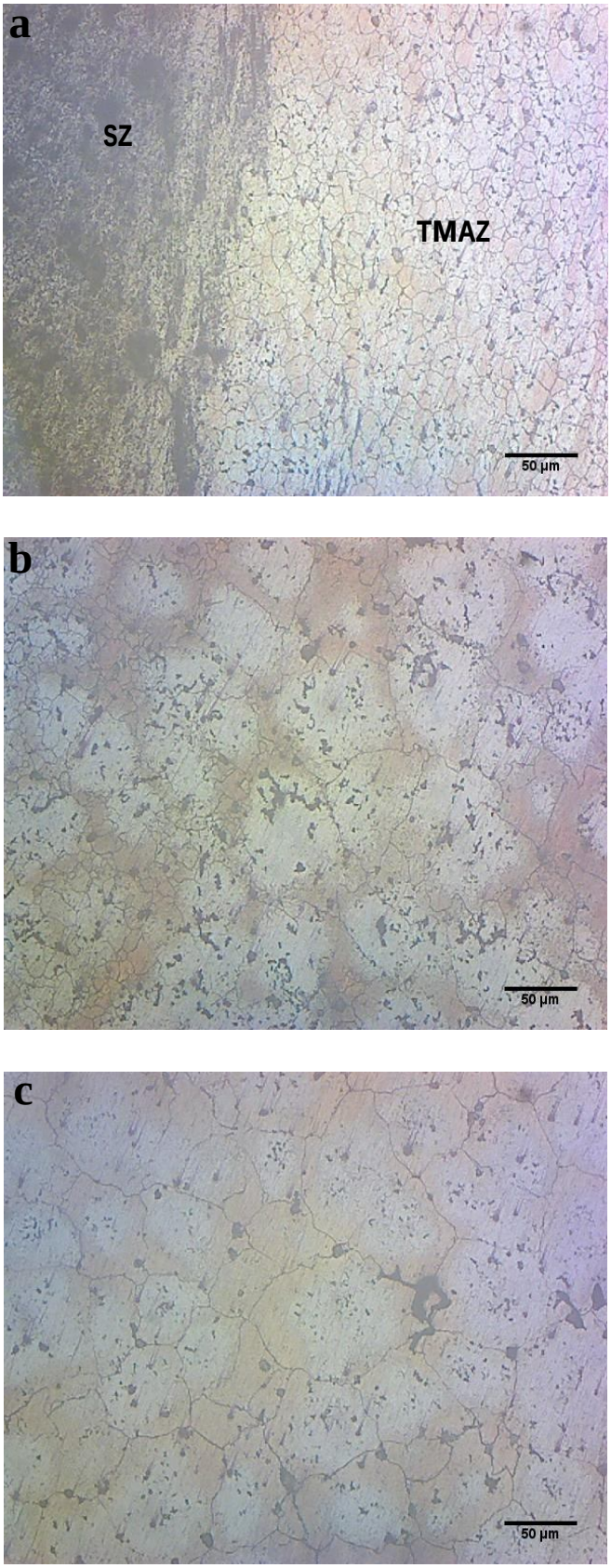

Figure 4.4 Various regions of FSPed H1 alloy with particle (a) Transition region, (b) TMAZ region and (c) HAZ region.

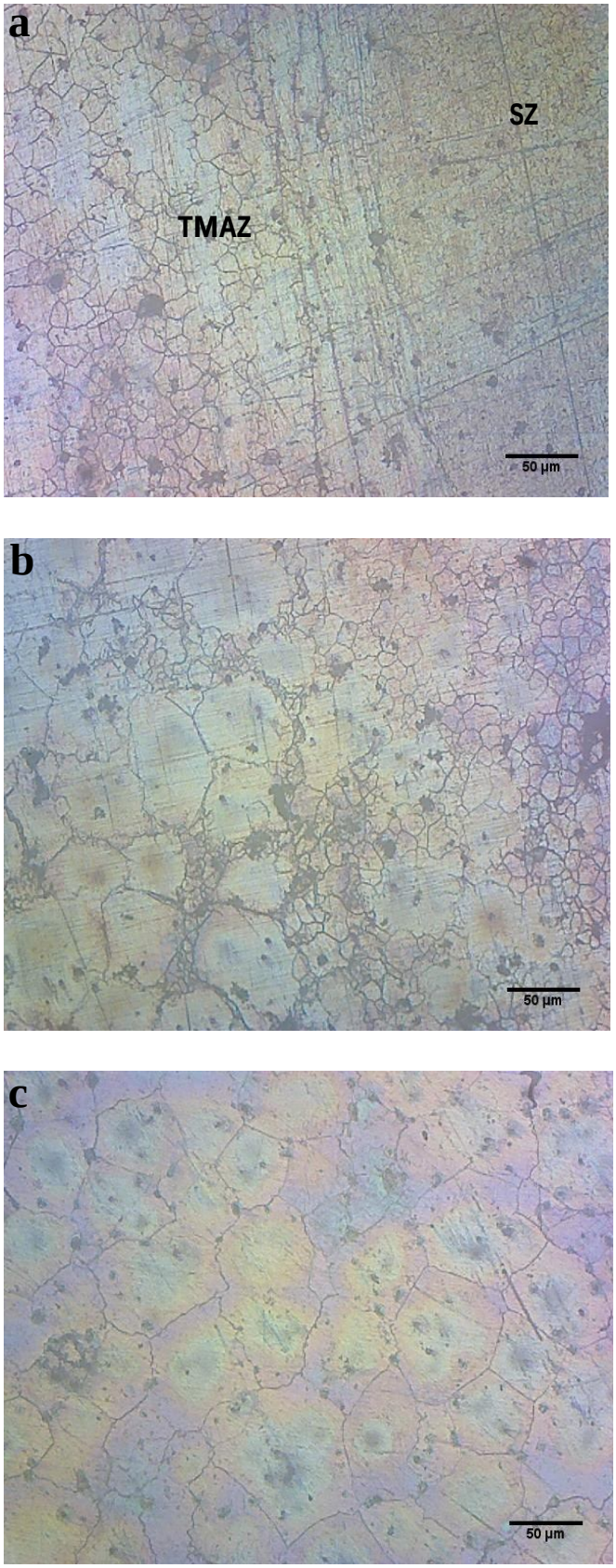

Figure 4.5 Various regions of FSPed H1 alloy without particle (a) Transition region, (b) TMAZ region and (c) HAZ region.

4.2 Microhardness

The average hardness of the base material was reported as 57 Hv by Gaurav et al. [47]. Six readings were taken (along the depth) in the stirred zone of the transverse cross-sectional of FSPed/H1 and H1/B_4C, and their average is reported. Table 4.1 presents average vicker's hardness value in Hv of all three H1 alloy types.

Table 4.1
Vicker's Hardness value of H1 alloy/B_4C surface composite.

H1 Alloy Condition	Designation	Hardness (Hv)
Base Metal	BM	57
FSPed without B_4C	FSPed/H1	92
FSPed with B_4C	H1/B_4C	101

As we can seen from the above results, FSP resulted in increase of hardness from 57 Hv to 92 Hv and further to 101 Hv by the incorporation of reinforcement particles. Increase of hardness due to FSP can be explained by Hall-Petch relationship. According to Hall-Petch relation:

$$\sigma_y = \sigma_i + kd^{0.5}$$

Here, 'σ_y' represents the yield strength of polycrystalline material, 'σ_i' represents the yield strength of same material at infinite grain size, 'k' represents hall-petch constant and'd' represents the average grain size. It is evident from above relation that grain size is inversely proportional to yield strength (or hardness). As grain size (d) decreases, there will be more number of Grain Boundaries (GBs) which leads to less movement of dislocation and restriction increases for slip movement and this ultimately results in increase of strength and hardness. FSP resulted in decrease of grain size due to grain refinement and pinning effect of B_4C particles, which resulted in increase of yield strength and ultimately leads to increase in hardness. Therefore, grain refinement is the common mechanism involved in increase of hardness for FSPed alloy with and without B_4C particle, while pinning effect of B_4C particles is an additional mechanism involved in increase of hardness for FSPed alloy with B_4C particle.

4.3 Wear Properties

The wear behavior of the as received H1 alloy, FSPed without particle and FSPed with particle (B_4C micro sized particle) was evaluated by a pin on disc tribometer. Wear test was conducted at two loads of 30 N and 10 N. Table 4.2 presents the complete wear test results, primarily mentioning wear rate (mg/m) and friction coefficient. Here, friction coefficient is calculated as the ratio of average friction force and load.

Table 4.2
Wear Test Results

H1 Alloy Condition	Load (N)	Weight loss (g)	Wear rate (mg/m)	Friction coefficient	Hardness (Hv)
Base Metal	30	0.0963	0.0321	0.26	57
FSPed without B_4C		0.0632	0.0211	0.22	92
FSPed with B_4C		0.0519	0.0173	0.19	101
FSPed without B_4C	10	0.0449	0.0149	0.22	92
FSPed with B_4C		0.0336	0.0112	0.19	101

Fig 4.6 represents the variation of weight loss (mg) with the sliding distance (m) for all the tested wear samples. The decreasing trend of wear rate from base metal to FSPed specimen with particle at 10 N is represented by the bar graph as shown in fig 4.7. It can be inferred from all results, that samples containing hard secondary phase B_4C particles in the Mg matrix exhibit less weight loss and wear rate as compared to the FSPed sample having no reinforcement particle and the parent metal. This is due to decrease in grain size of the FSPed alloy. Moreover, samples tested at 10 N load exhibited less wear rate and weight loss

compared to 30 N load samples. Therefore, FSPed sample with particle tested at 10 N exhibited least weight loss and wear rate as compared to other five samples. Fig 4.8 shows the comparison of wear rate (of the samples tested at 30 N) and microhardness of the corresponding samples. This variation clearly supports the Archard Equation [48] which is given by:

$$W = kLP/3H$$

where W is volume of materials worn out, k is the wear coefficient, L is the sliding distance, P the applied load and H is the bulk hardness of the materials. It can be inferred from above equation that wear rate is inversely proportional to hardness. This indicates that sample having less hardness will have more wear rate and vice-versa. Therefore, base metal was found to be having more wear rate as compared to the FSPed samples with and without particle. Now, it is evident from above discussion that FSPed alloy with reinforcement particle has shown better wear resistance, at both loads of 30 N and 10 N, compared to BM and FSPed/H1. The variation of friction coefficient with sliding distance at an applied load of 30 N is shown in fig 4.9 for BM and fig 4.10 for FSPed/H1 and H1/B_4C. The as-cast H1 alloy has shown higher value of friction coefficient compared to other two conditions of H1 alloy. This is due to the presence of hard reinforcenemnt particles B_4C present in the FSPed H1/B_4C composite (as confirmed by XRD results) which decreases the direct load, thus reducing friction coefficient. Moreover, these B_4C particles act as lubricant, thus reducing friction coefficient. Also, as load is decreased from 30 N to 10 N, friction coefficient remains almost constant for both FSPed H1 alloy with and without particle specimen as shown in fig 4.11.

4.3.1 Wear Mechanism

In order to investigate the wear mechanism, worn surfaces of the wear samples were examined under SEM. The worn out surfaces of the pin materials show diverse topographical features. The worn out surfaces of all the specimens tested were covered with grooves parallel to the sliding direction. Worn surface of the base metal at an applied load of 30 N is shown in fig 4.12. It can be observed that worn surface is characterized by the long continuous grooves, microcutting and fractured surface which indicates that abrasion is the dominant wear mechanism in case of base metal. Further, adhesion wear can also be observed from the worn surface of base metal since material transfer is evident on the worn surfaces there are also signs of smearing and plastic deformation. Numerous shallow grooves and scratch marks were observed in the SEM micrograph of worn out surface of FSPed/H1 alloy

tested at 30 N as shown in fig 4.13. Such features are characteristics of abrasion in which hard asperities on the steel counterface, or hard particles in between the contacting surfaces, plough or cut into the pin, causing wear by the removal of small fragments. Moreover, fractured particles were also observed, this can be due to the application of high load. Worn surface of the H1/B_4C composite tested at 30 N (shown in fig 4.14) is characterized by the shallow grooves and ploughing marks indicating abrasion mechanism. Surface oxidation is also observed due to the presence of oxide layer on the worn surface. At some areas of worn surfaces as shown at higher magnification in fig 4.14, some traces of material removal in the form of platelets were also observed which indicates the presence of delamination wear mechanism. Thus, abrasion and oxidation were observed to be the major wear mechanisms at 30 N load with some involvement of surface delamination. As the load is decreased from 30 N to 10 N, shallow grooves characterization changes into deep grooves for both FSPed/H1 and H1/B_4C as shown in fig. 4.15 and 4.16. Moreover, fractured particles and traces of delamination were observed in the worn surface of FSPed/H1 as shown in fig 4.15.

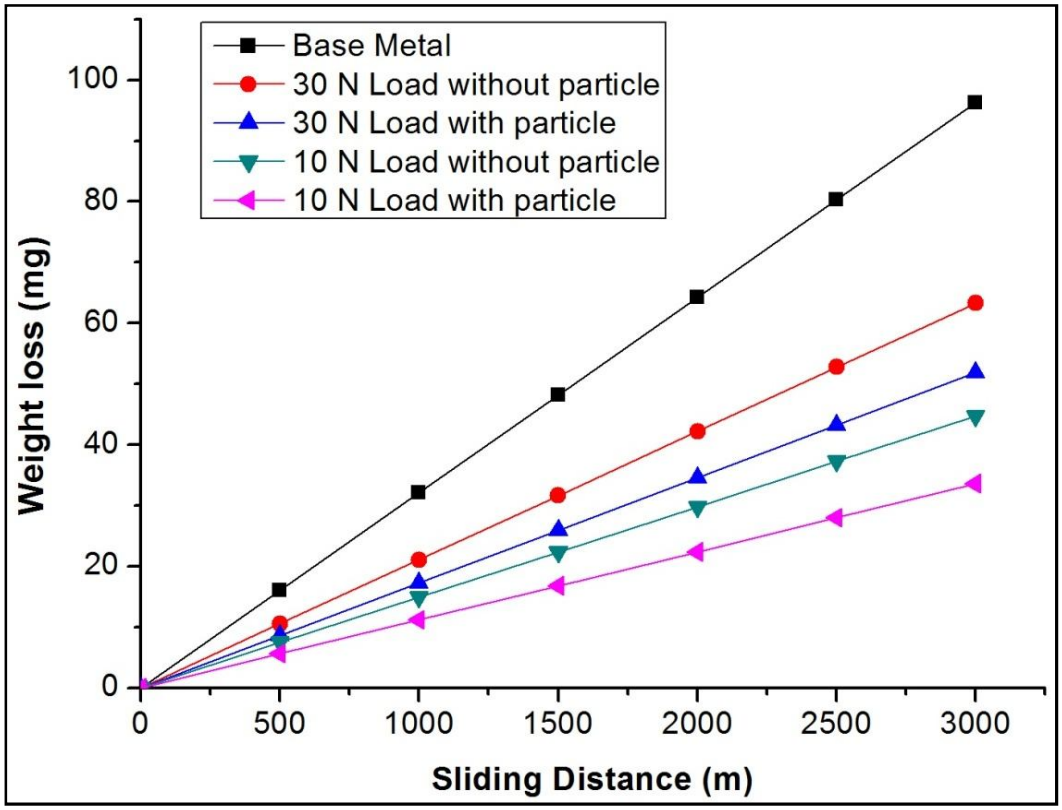

Figure 4.6 Variation of weight loss (mg) with the sliding distance (m) for the base metal, FSPed/H1 and H1/B_4C.

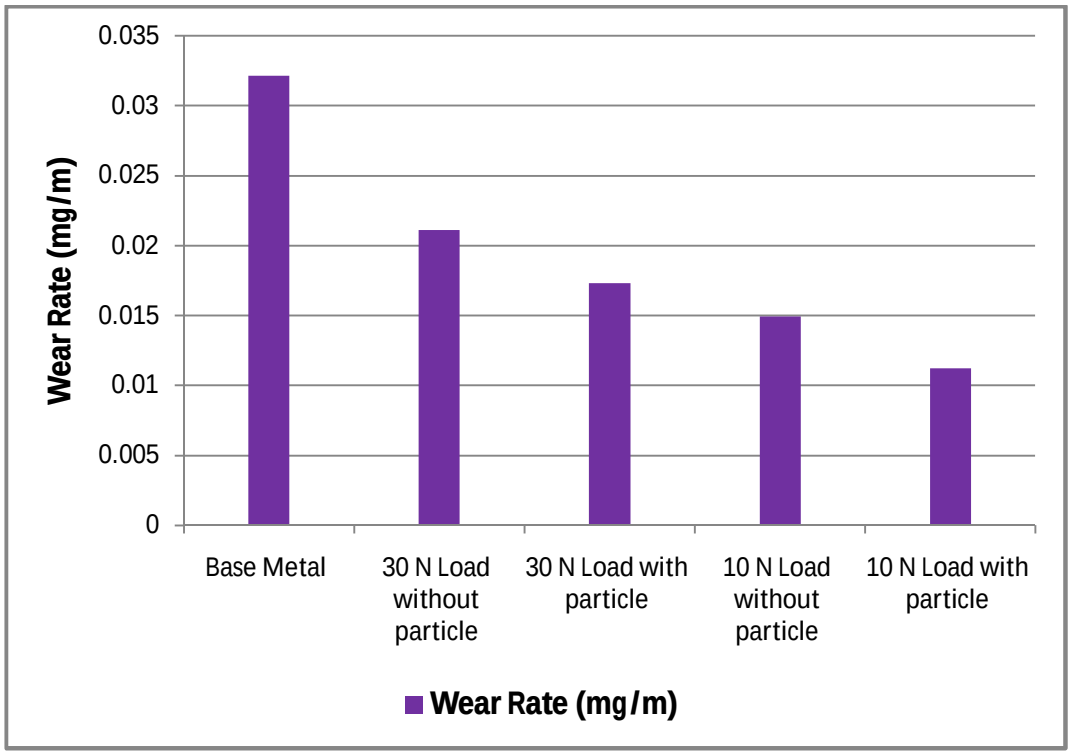

Figure 4.7 Wear rate trend (mg/m) for all tested samples.

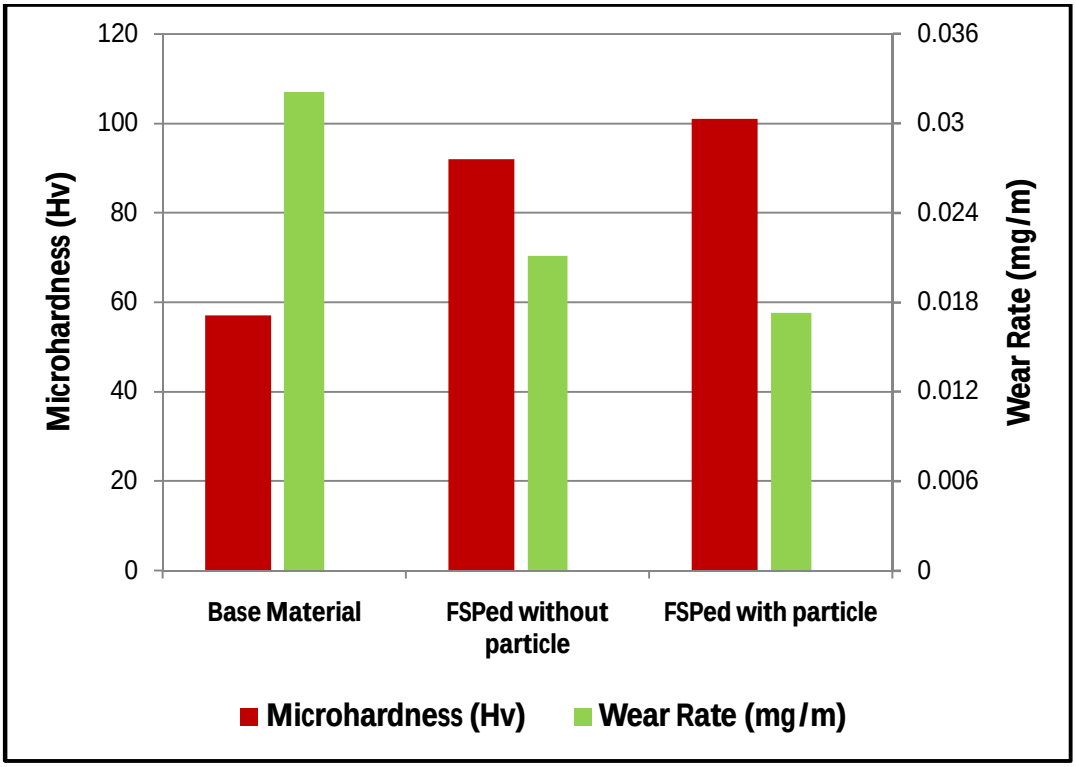

Figure 4.8 Wear rate Vs Microhardness.

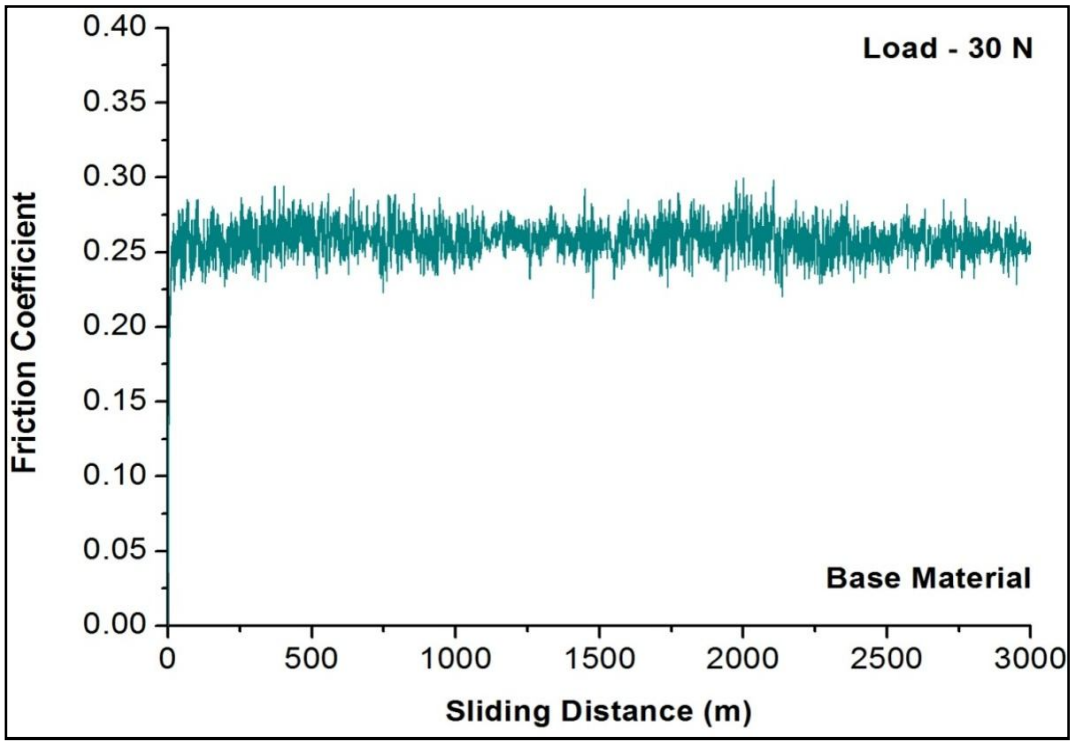

Figure 4.9 Variation of Friction Coefficient with Sliding Distance at 30 N load for Base metal (BM).

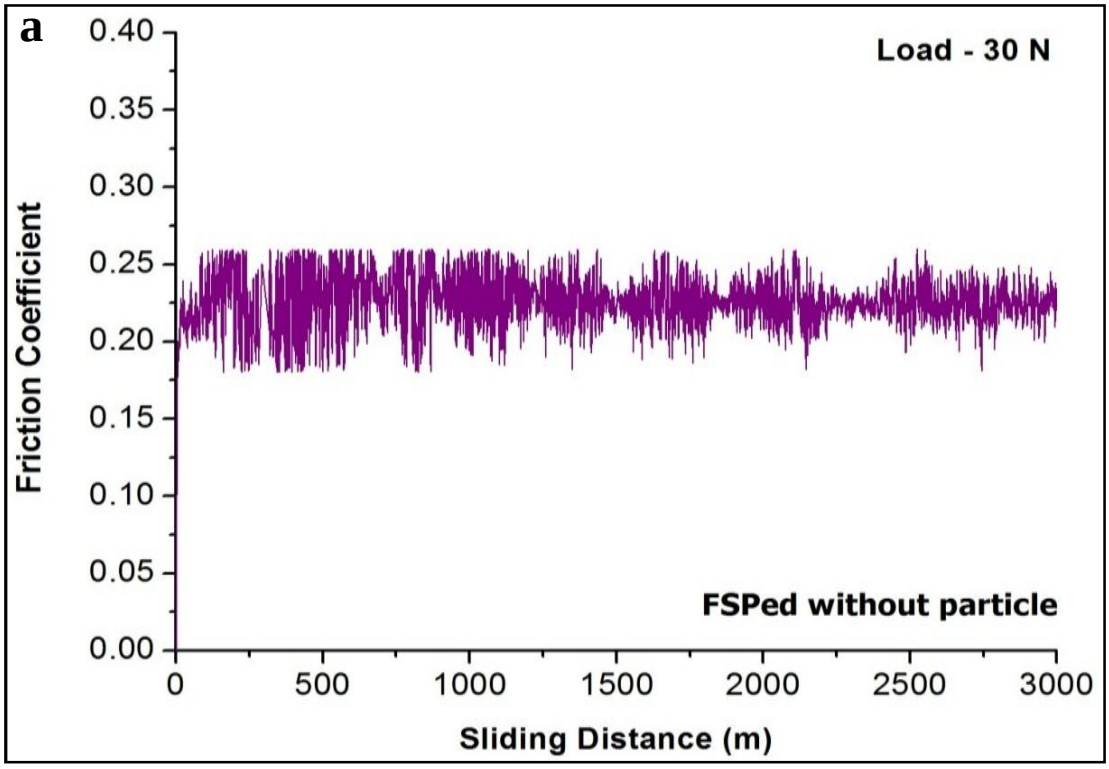

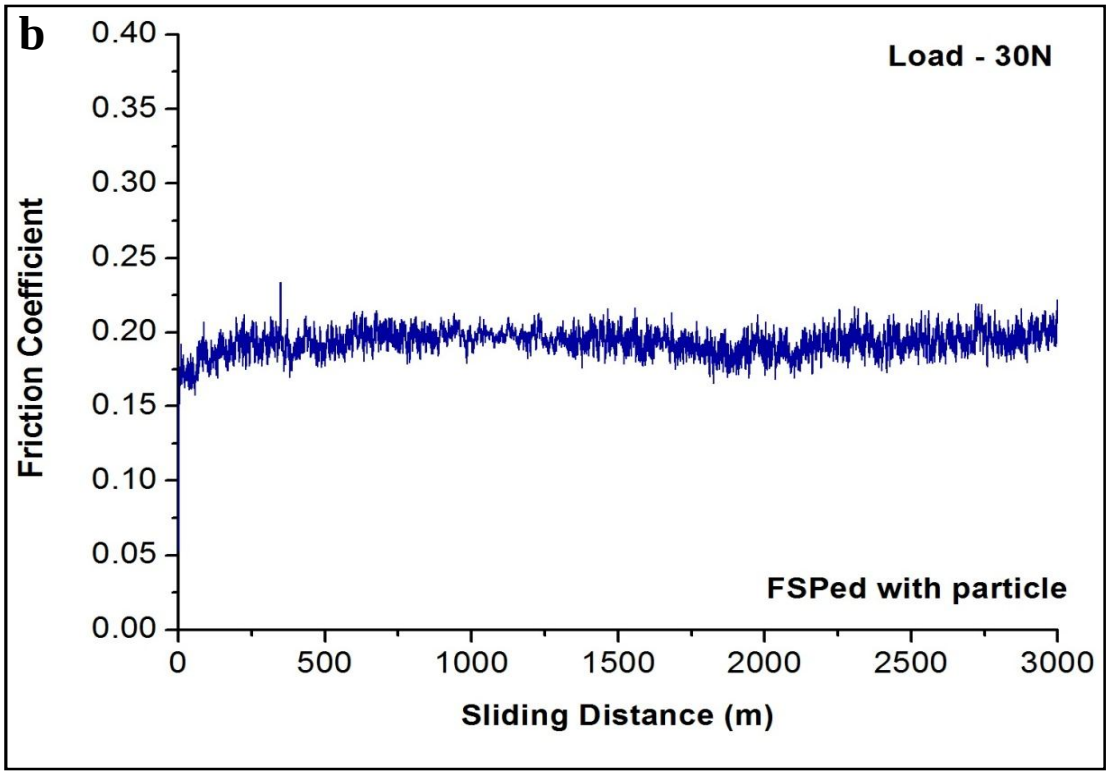

Fig 4.10 Variation of Friction Coefficient with Sliding Distance at 30 N load for (a) FSPed/H1and (b) H1/B_4C.

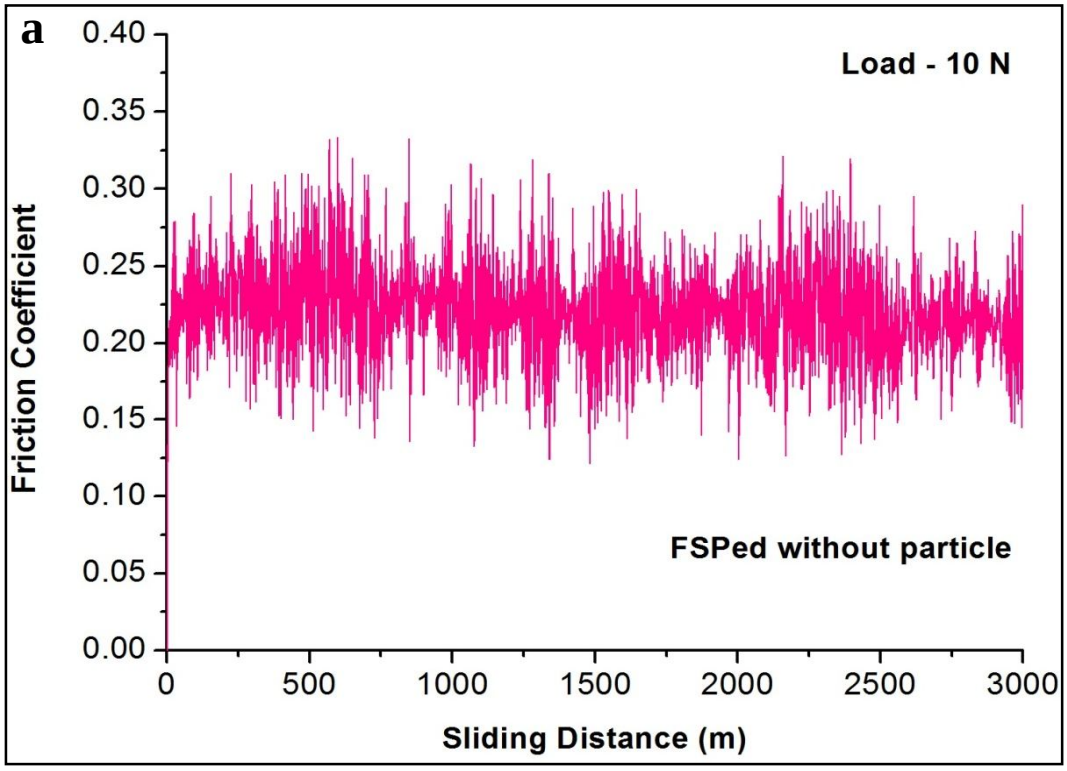

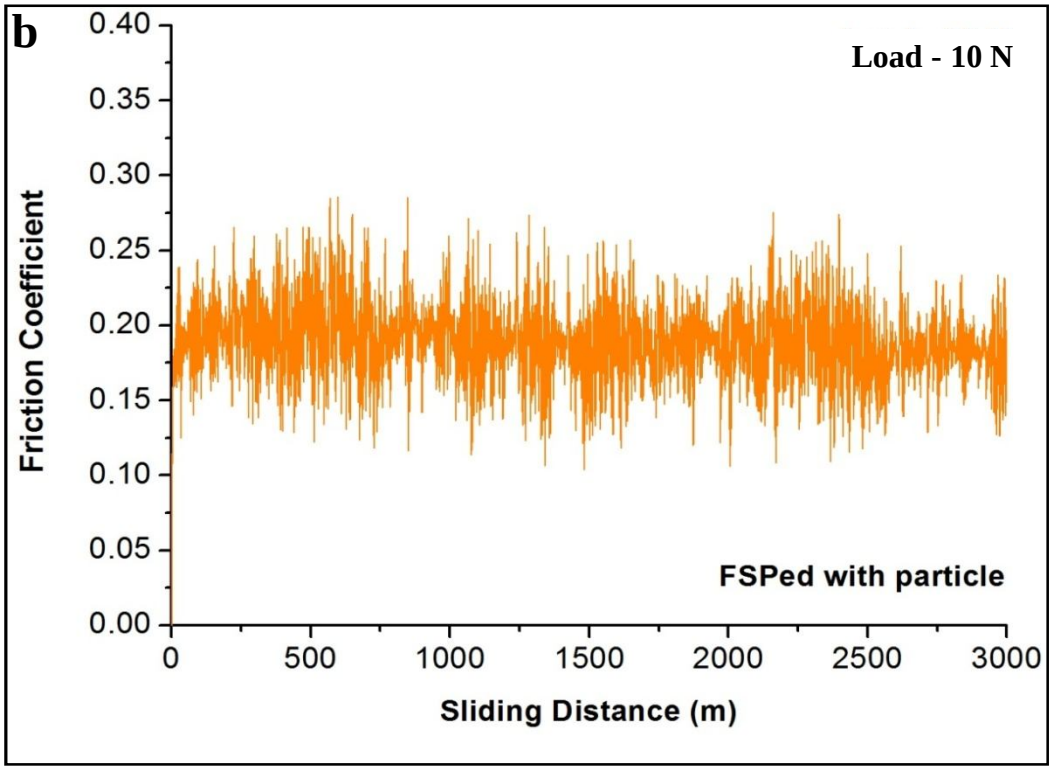

Fig 4.11 Variation of Friction Coefficient with Sliding Distance at 10 N load for (a) FSPed/H1 and (b) H1/B_4C.

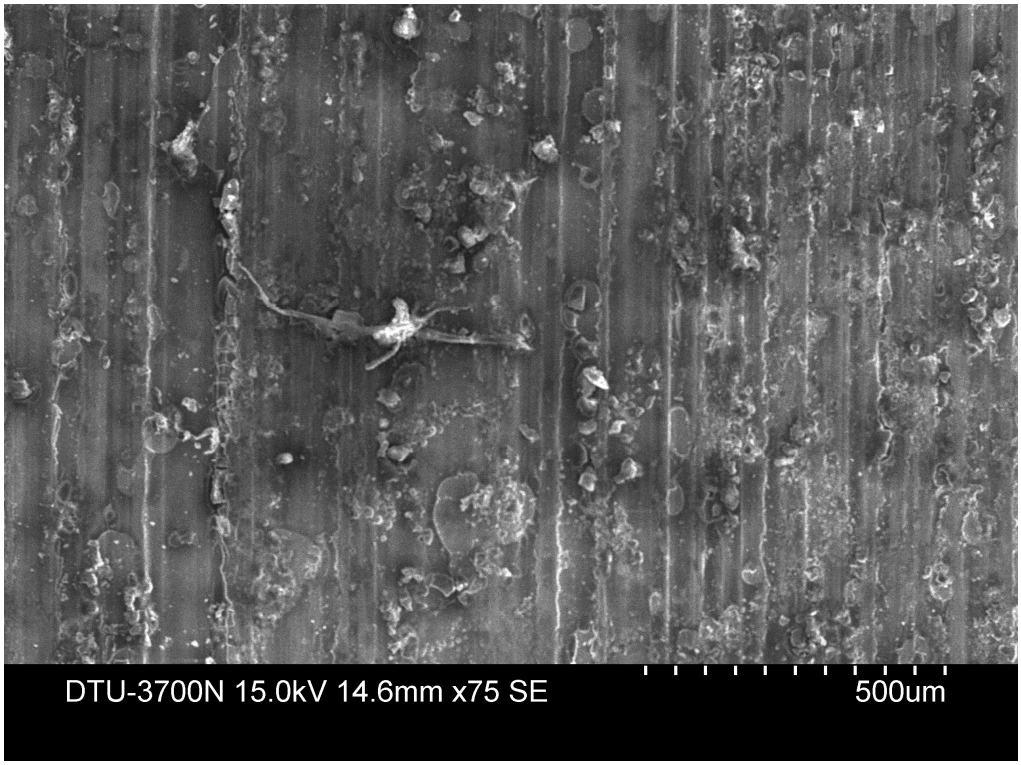

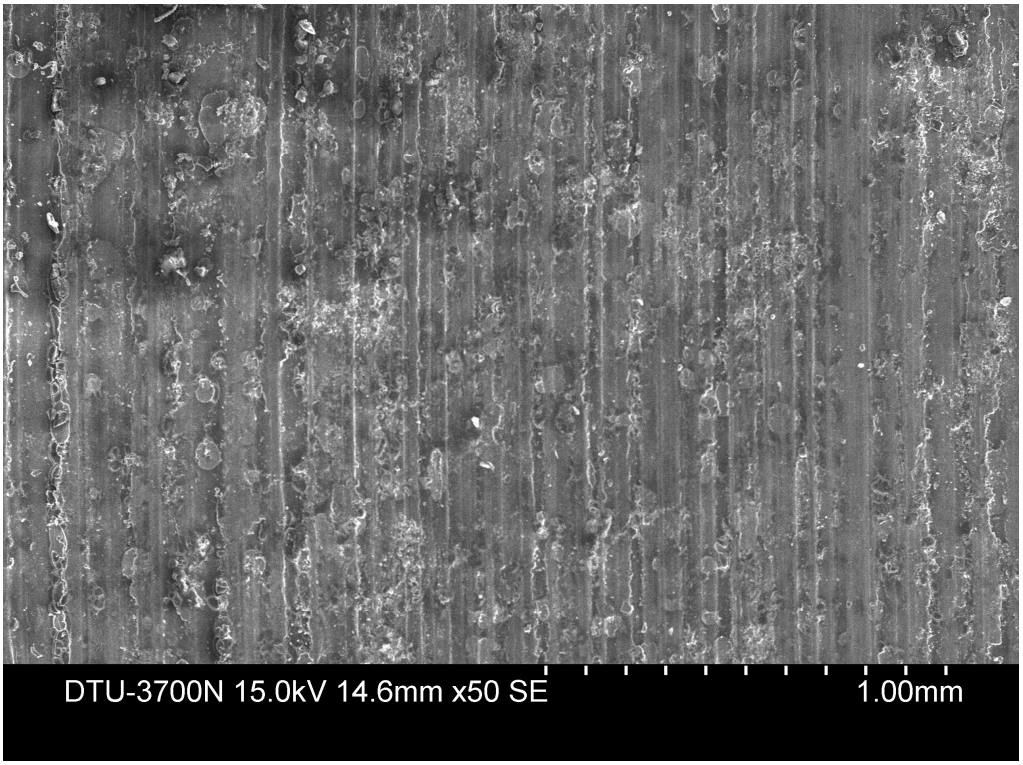

Figure 4.12 SEM micrograph of the worn out surface of BM at an applied load of 30 N.

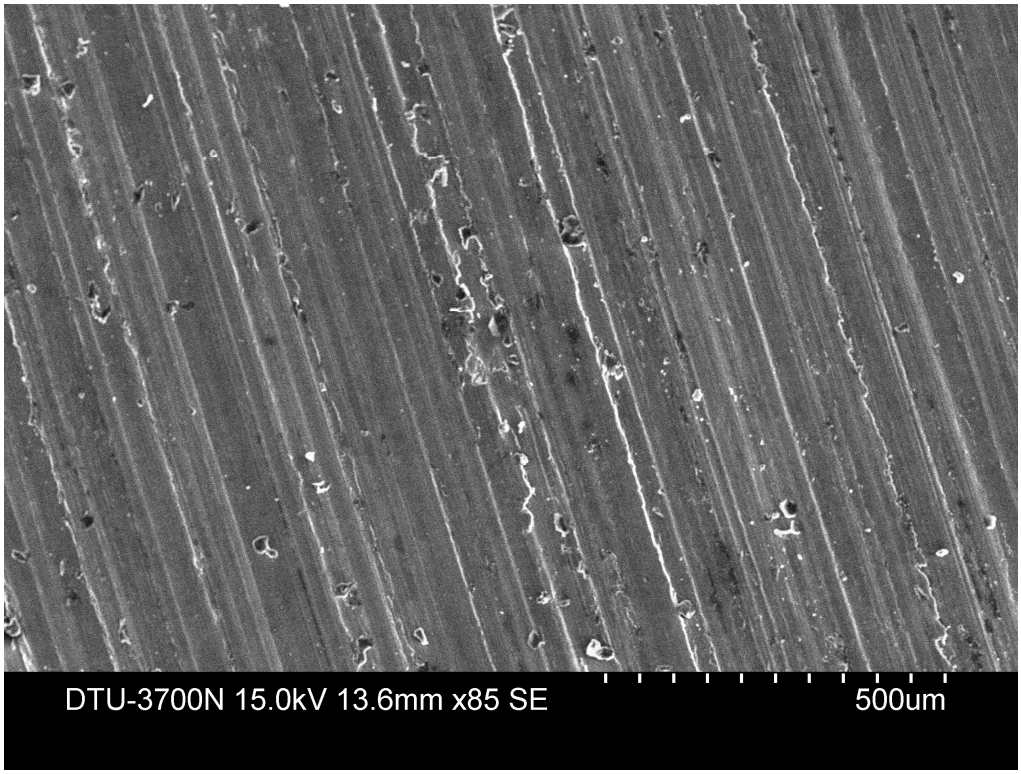

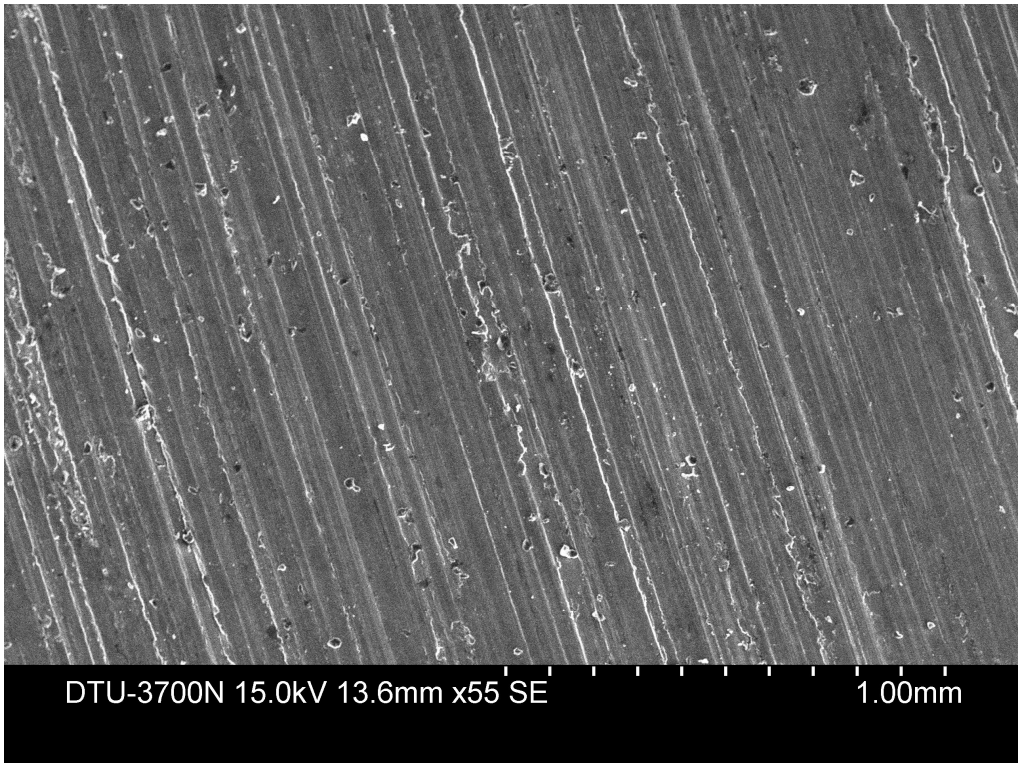

Figure 4.13 SEM micrograph of the worn out surface of FSPed alloy without B_4C at an applied load of 30 N.

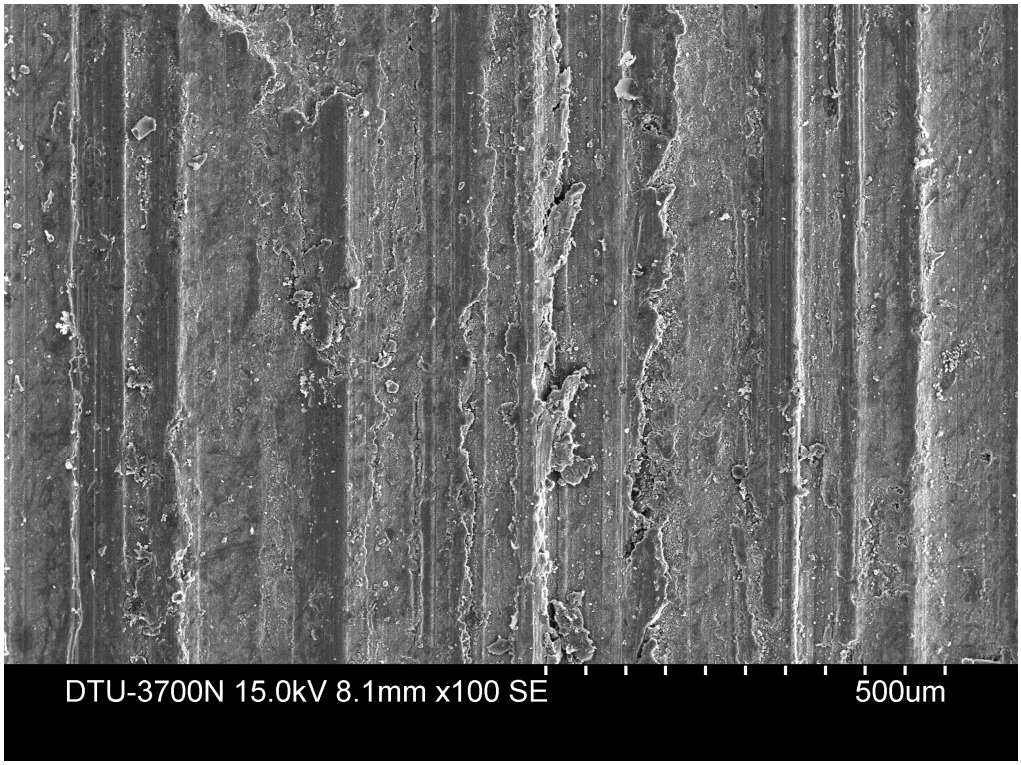

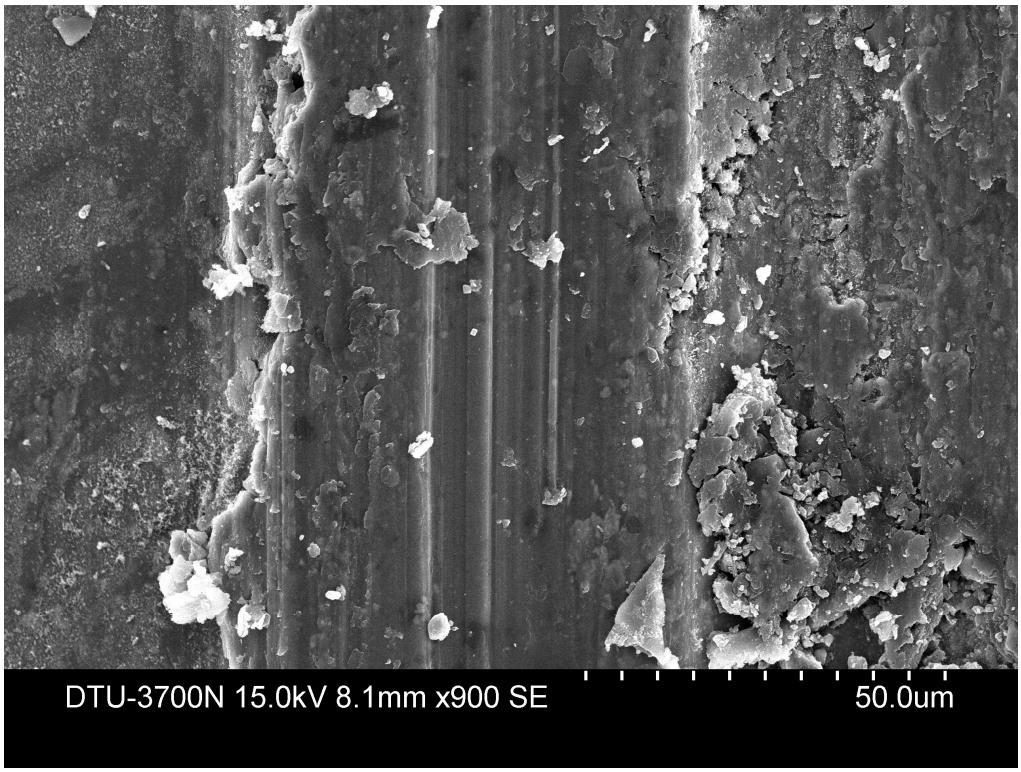

Figure 4.14 SEM micrograph of the worn out surface of FSPed alloy with B_4C at an applied load of 30 N.

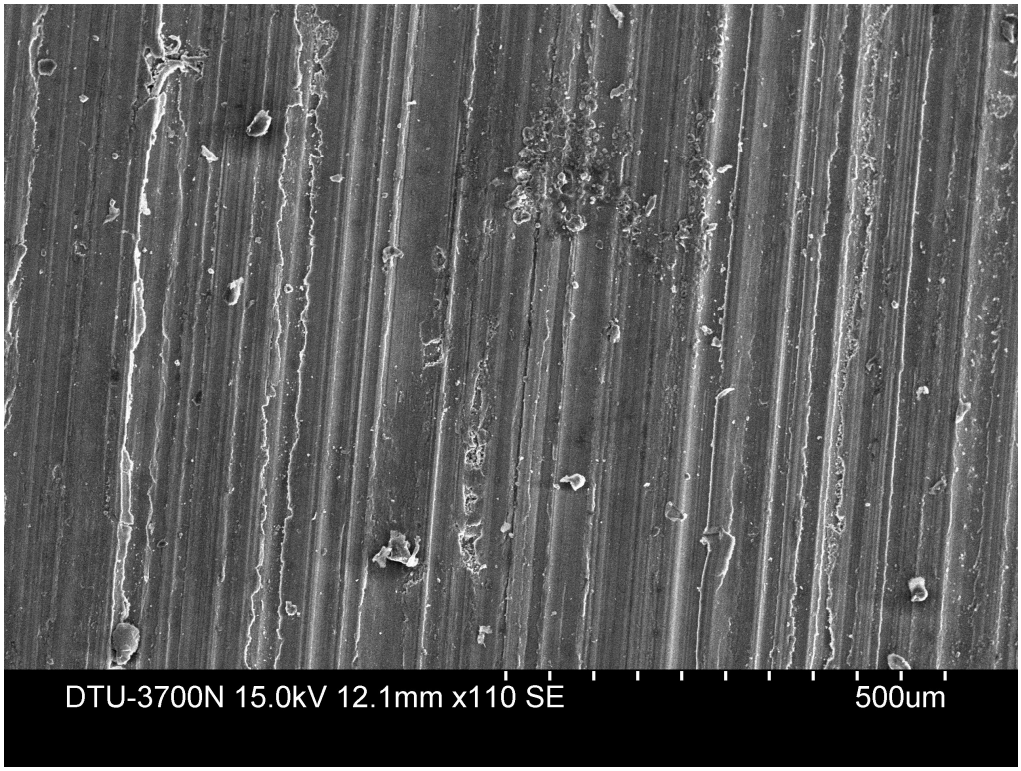

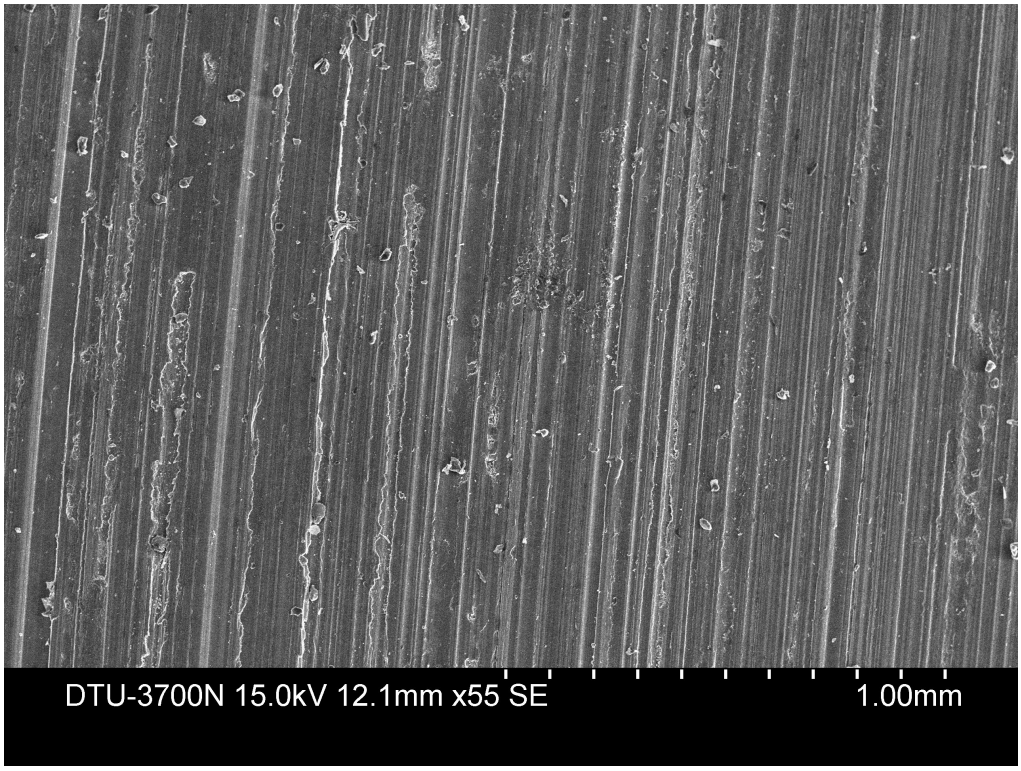

Figure 4.15 SEM micrograph of the worn out surface of FSPed alloy without B_4C at an applied load of 10 N.

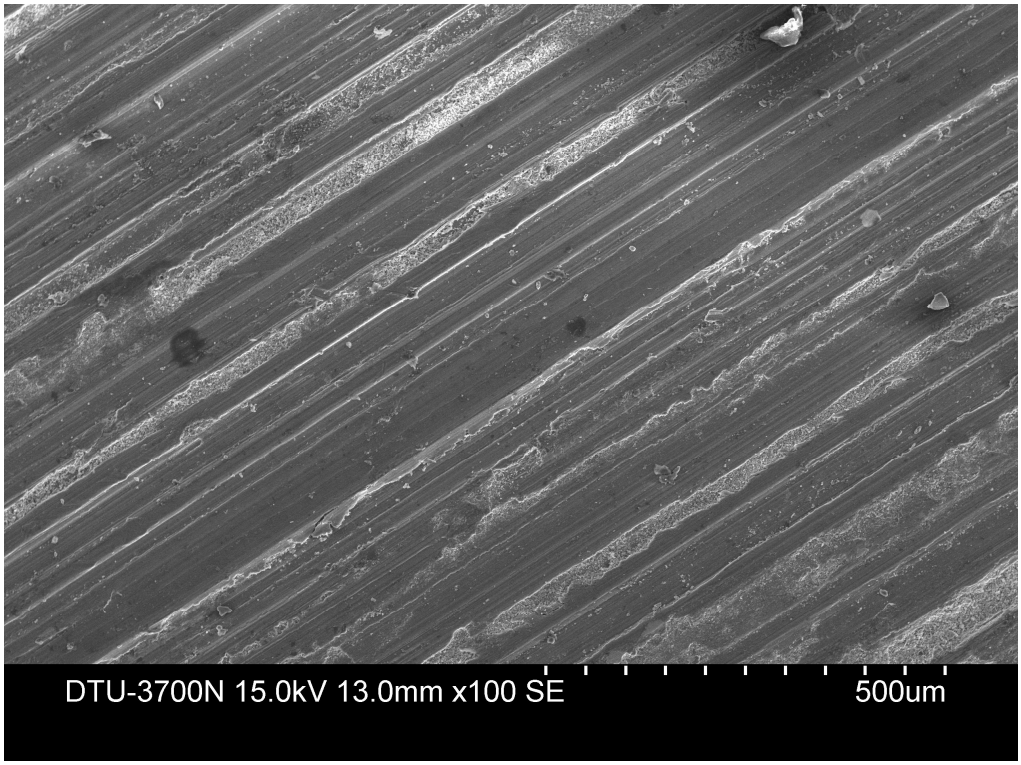

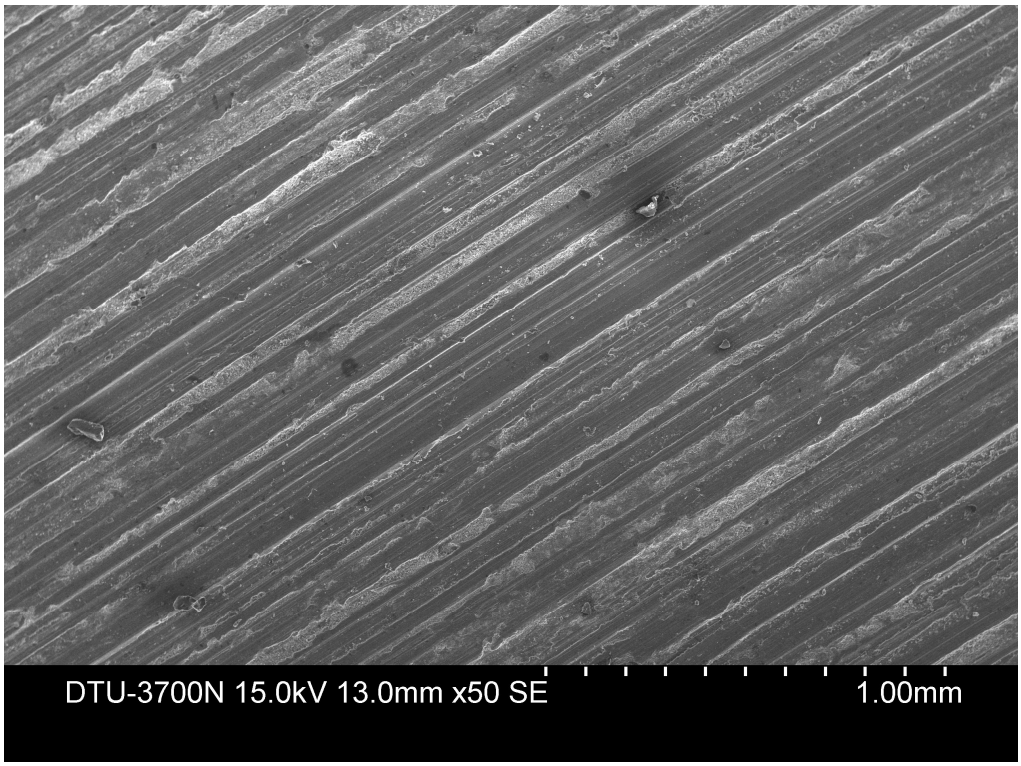

Figure 4.16 SEM micrograph of the worn out surface of FSPed alloy with B_4C at an applied load of 10 N.

CHAPTER-5

CONCLUSIONS

Magnesium alloy having composition Mg-4Al-3Zn-3Pb-3Sn-0.5misch metal (MM), designated as H1 alloy and Boron Carbide (B_4C) surface composite was successfully synthesized using the novel method of FSP without any formation of defects. Effect of reinforcement particle on the microstructure, microhardness and wear properties of the surface composite produced was investigated by performing various tests on the sample. Following were the major findings:

1. FSP resulted in significant grain refinement of particles and uniform distribution of B_4C particles in the magnesium matrix. Pinning effect of reinforcement particles and grain refinement leads to reduction in grain size.
2. FSPed H1 alloy with B_4C particle exhibited higher hardness of 101 Hv as compared to 92 Hv of FSPed H1 alloy without B_4C and 57 Hv of the parent metal due to reduction in grain size as explained by Hall-Petch relationship.
3. FSPed H1 alloy with B_4C particle exhibited least wear rate of 0.0173 mg/m in case of 30 N applied load while 0.0112 mg/m in case of 10 N applied load. Also, H1/B_4C exhibited least friction coefficient of 0.19 (both 30 N and 10 N load) compared to base metal and FSPed H1 alloy without particle. This shows that addition of B_4C particles resulted in improved wear resistance of Mg based alloy (H1 alloy) compared to the parent metal.
4. As the load increases, wear rate was found to be increasing but friction coefficient remains almost constant. Abrasion mechanism was the dominating mechanism in all the tested sample since all samples are characterized by ploughing and groove marks parallel to the sliding direction.

REFERENCES

[1] B.L. Mordike and T. Ebert "**Magnesium Properties — applications — potential"** Materials Science and Engineering A302 (2001) 37–45.

[2] Ma Qian and A. Das **"Grain refinement of magnesium alloys by zirconium: Formation of equiaxed grains"** Scripta Materialia 54 (2006) 881-886.

[3] J. Cai, G.C. Ma, Z. Liu, H.F. Zhang, Z.Q. Hu **"Influence of rapid solidification on the microstructure of AZ91HP alloy"** Journal of Alloys and Compounds 422 (2006) 92–96.

[4] K. Mathis, J. Gubicza, N.H. Nam **"Microstructure and mechanical behavior of AZ91 Mg alloy processed by equal channel angular pressing"** Journal of Alloys and Compounds 394 (2005) 194-199.

[5] A.A. Luo, and M.O. Pekguleryz **"Cast Magnesium Alloys for elevated temperature applications"** Journal of Materials Science 29 (1994) 5259-527.

[6] R.S. Mishra and Z.Y. Ma **"Friction Stir Welding and Processing"** Materials Science and Engineering R 50 (2005) 1 – 78.

[7] A.H. Feng and Z.Y. Ma **"Enhanced mechanical properties of Mg–Al–Zn cast alloy via friction stir processing"** Scripta Materialia 56 (2007) 397–400.

[8] R.S. Mishra, Z.Y. Ma, I. Charit **"Friction stir processing: a novel technique for fabrication of surface composite"** Materials Science and Engineering A341 (2003) 307–310.

[9] Z.Y. Ma, R.S. Mishra, M.W. Mahoney "**Superplastic deformation behaviour of friction stir processed 7075Al alloy"** Acta Materialia 50 (2002) 4419–4430.

[10] Vipin Sharma, Ujjwal Prakash, B.V. Manoj Kumar **"Surface composites by friction stir processing: A review"** Journal of Materials Processing Technology 224 (2015) 117–134.

[11] Abhijit Dey and Krishna Murari Pandey **"Magnesium Metal Matrix Composites- A Review"** Reviews on Advanced Materials Science 42 (2015) 58-67.

[12] Hai Zhi Ye and Xing Yang Liu **"Review of recent studies in magnesium matrix composites"** Journal of Materials Science 39 (2004) 6153 – 6171.

[13] B.M. Darras, M.K. Khraisheh, F.K. Abu-Farha, M.A. Omar **"FSP of commercial AZ31 magnesium alloy"** Journal of Materials Processing Technology 191 (2007) 77–81.

[14] Wang Wen, Wang Kuaishe, Guo Qiang, Wu Nan **"Effect of Friction Stir Processing on Microstructure and Mechanical Properties of Cast AZ31 Magnesium Alloy"** Rare Metal Materials and Engineering 2012, 41(9): 1522-1526.

[15] J.A. del Valle, P.Rey, D.Gesto, D.Verdera, J.A. Jiménez, O.A. Ruano **"Mechanical properties of ultra-fine grained AZ91 magnesium alloy processed by friction stir processing"** Materials Science & Engineering A628 (2015) 198–206.

[16] DU Xing-hao and WU Bao-lin **"Using friction stir processing to produce ultrafine-grained microstructure in AZ61 magnesium alloy"** Transactions of Nonferrous Metals Society of China 18(2008) 562-565.

[17] S. Ramesh Babu , V.S. Senthil Kumar, G. Madhusudhan Reddy, L Karunamoorthy **"Microstructural changes and mechanical properties of friction stir processed extruded AZ31B alloy"** Procedia Engineering 38 (2012) 2956 – 2966.

[18] H.S. Arora, H.Singh, B.K.Dhindaw, "**Wear behaviour of a Mg alloy subjected to friction stir processing"** Wear 303 (2013) 65–77.

[19] Genghua Cao, Datong Zhang , Wen Zhang, Cheng Qiu **"Microstructure evolution and mechanical properties of Mg–Nd–Y alloy in different friction stir processing conditions"** Journal of Alloys and Compounds 636 (2015) 12–19.

[20] F.Y. Zheng, Y.J. Wu, L.M. Peng, X.W. Li, P.H. Fu, W.J. Ding **"Microstructures and mechanical properties of friction stir processed Mg-2.0Nd-0.3Zn-1.0Zr magnesium alloy"** Journal of Magnesium and Alloys 1 (2013) 122-127.

[21] N. Saini, D.K. Dwivedi, P.K. Jain, H. Singh **"Surface Modification of Cast Al-17%Si Alloys using Friction Stir Processing"** Procedia Engineering 100 (2015) 1522 – 1531.

[22] S. Chainarong, P. Muangjunburee, S. Suthummanon **"Friction Stir Processing of SSM356 Aluminium Alloy"** Procedia Engineering 97 (2014) 732 – 740.

[23] L. Karthikeyan, V.S. Senthilkumar, V. Balasubramanian, S. Natarajan **"Mechanical property and microstructural changes during friction stir processing of cast aluminum 2285 alloy"** Materials and Design 30 (2009) 2237–2242.

[24] S.M. Aktarer, D.M.Sekban, O.Saray, T.Kucukomeroglu, Z.Y.Ma, G.Purcek **"Effect of two pass friction stir processing on the microstructure and mechanical properties of as-cast binary Al–12 Si alloy"** Materials Science & Engineering A636 (2015) 311–319.

[25] T.S. Mahmoud and S.S.Mohamed **"Improvement of microstructural, mechanical and tribological characteristics of A413 cast Al alloys using friction stir processing"** Materials Science & Engineering A558 (2012) 502–509.

[26] Y. Morisada, H. Fujii, T. Nagaoka, M. Fukusumi **"MWCNTs/AZ31 surface composites fabricated by friction stir processing"** Materials Science and Engineering A 419 (2006) 344–348.

[27] Y. Morisada, H. Fujii, T. Nagaoka, M. Fukusumi **"Effect of friction stir processing with SiC particles on microstructure and hardness of AZ31 Y"** Materials Science and Engineering A 433 (2006) 50–54.

[28] C.J. Lee, J.C. Huang, P.J. Hsieh **"Mg based nano-composites fabricated by friction stir processing"** Scripta Materialia 54 (2006) 1415–1420.

[29] M. Dadashpour, A.Mostafapour, R.Yeşildal, S.Rouhi **"Effect of process parameter on mechanical properties and fracture behavior of AZ91C/SiO_2 composite fabricated by FSP"** Materials Science & Engineering A655 (2016) 379–387.

[30] Mohammad Navazania and Kamran Dehghani **"Fabrication of Mg-ZrO_2surface layer composites by friction stir processing"** Journal of Materials Processing Technology 229 (2016) 439–449.

[31] Mohammad Navazania and Kamran Dehghani **"Investigation of microstructure and hardness of Mg/TiC Surface Composite Fabricated by Friction Stir Processing (FSP)"** Procedia Materials Science 11 (2015) 509-514.

[32] M. Balakrishnan, I. Dinaharan, R. Palanivel, R. Sivaprakasam **"Synthesize of AZ31/TiC magnesium matrix composites using friction stir processing"** Journal of Magnesium and Alloys 3 (2015) 76-78.

[33] Yupei Jiang, XuyueYang, Hiromi Miura, Taku Sakai **"Nano-SiO_2 particles reinforced Mg Alloy Produced FSP"** Reviews on Advanced Materials Science 33 (2013) 29-32.

[34] P. Asadi, M.K. Besharati Givi, G. Faraji "**Producing Ultrafine-Grained AZ91 from As-Cast AZ91 by FSP"** Mater. Manuf. Process. 25 (2010) 1219–1226.

[35] D. Khayyamin, A. Mostafapour, R. Keshmiri **"The effect of process parameters on microstructural characteristics of AZ91/SiO_2 composite fabricated by FSP"** Materials Science & Engineering A559 (2013) 217–221.

[36] Y. Erfan and S.F. Kashani-Bozorg **"Fabrication of Mg/SiC nanocomposite surface composite layer using FSP technique"** International Journal of Nano science 10 (2011) 1073.

[37] K. Sun, Q.Y. Shi, Y.J. Sun, G.Q. Chen "**Microstructure and mechanical property of nano-SiCp reinforced high strength Mg bulk composites produced by friction stir processing"** Materials Science and Engineering A 547 (2012) 32– 37.

[38] Parviz Asadi, Ghader Faraji, Mohammad K. Besharati **"Producing of AZ91/SiC composite by friction stir processing (FSP)"** International Journal of Advanced Manufacturing Technology 51 (2010) 247–260.

[39] M. Azizieh, A.H. Kokabi, P. Abachi "**Effect of rotational speed and probe profile on microstructure and hardness of AZ31/Al_2O_3 nano composites fabricated by friction stir processing"** Materials and Design 32 (2011) 2034–2041.

[40] Ghader Faraji and Parviz Asadi "**Characterization of AZ91/alumina nanocomposite produced by FSP"** Materials Science and Engineering A528 (2011) 2431–2440.

[41] Dehong Lu, Yehua Jiang, Rong Zhou **"Wear performance of nano-Al_2O_3 particles and CNTs reinforced magnesium matrix composites by friction stir processing"** Wear 305 (2013) 286–290.

[42] G. Madhusudhan Reddy, Sambasiva Rao, K. Srinivasa Rao **"Friction Stir Processing for Enhancement of Wear Resistance of ZM21 Magnesium Alloy"** Transactions of the Indian Institute of Metals 66(1) (2013) 13–24.

[43] T. Chen, Z. Zhu, Y. Ma, Y. Li, Y. Hao, J.Wuhan, **"Friction stir processing of thixoformed AZ91D magnesium alloy and fabrication of surface composite reinforced by SiC_ps"** Journal of Wuhan University of Technology – Material Science Edition (2010) 223–227.

[44] A. Mertens, A. Simar, J. Adrien, E. Maire, H.-M. Montrieux, F. Delannay, et al., **"Influence of fibre distribution and grain size on the mechanical behaviour of friction stir processed Mg–C composites"** Mater. Charact. 107 (2015) 125–133.

[45] A. Mertens, A. Simar, H.M. Montrieux, J. Halleux, F. Delannay, J. Lecomte-Beckers, W.J. Poole, K.U. Kainer (Eds.) "**Friction stir processing of magnesium matrix composites reinforced with carbon fibres: Influence of the matrix characteristics and of the processing parameters on microstructural developments"** Proceedings of the 9th International Conference on Magnesium Alloys and Their Apllications, Vancouver, Canada (2012) 845–850.

[46] Y. Huang, T. Wang, W. Guo, L. Wan, S. Lv, **"Microstructure and surface mechanical property of AZ31 Mg/SiC_p surface composite fabricated by Direct Friction Stir Processing"** Materials and Design 59 (2014) 274–278.

[47] G Gaurav, Q Murtaza, N Yuvraj, D Mandal, KL Sahoo and L Murmu **"Synthesis and effect of Misch metal on mechanical properties of conventional cast Mg–Al–Zn–Sn–Pb alloy system"** Proc IMechE Part L: Journal of Materials: Design and Applications 0(0) (2015).

[48] J.F. Archard **"Mechanics of subsurface void nucleation in delamination wear"** Journal of Applied Physics 24 (1953) 981-988.